

Distributed Beamforming for Spectrum-Sharing Systems With AF Cooperative Two-Way Relaying

Ali Afana, Ali Ghayeb, Vahid Asghari, and Sofiène Affes

Abstract—We consider in this paper distributed beamforming for two-way cognitive radio networks in an effort to improve the spectrum efficiency and enhance the performance of the cognitive (secondary) system. In particular, we consider a spectrum sharing system where a set of amplify-and-forward (AF) relays are employed to help a pair of secondary transceivers in the presence of multiple licensed (primary) users. The set of relays participate in the beamforming process, where the optimal beamformer weights are obtained via a linear optimization method. For this system, we investigate the transmission protocols over two and three time-slots. To study and compare the performance tradeoffs between the two transmission protocols, for both of them, we derive closed-form expressions for the cumulative distribution function (CDF) and the moment generating function (MGF) of the equivalent end-to-end signal-to-noise ratio (SNR) at the secondary receiver. We analyze the performance of the proposed methods where closed-form expressions for the user outage probability and the average error probability are derived for independent and identically distributed Rayleigh fading channels. Numerical results demonstrate the efficacy of beamforming in enhancing the secondary system performance in addition to mitigating the interference to the primary users. In addition, our results show that the three time-slot protocol outperforms the two time-slot protocol in certain scenarios where it offers a good compromise between bandwidth efficiency and system performance.

Index Terms—Cognitive radio, performance analysis, spectrum sharing systems, two-way cooperative relaying, zero forcing beamforming.

I. INTRODUCTION

SCARCITY and under-utilization of the spectrum usage necessitate exploiting the available spectrum opportunistically. Cognitive radio (CR), as an emerging solution, offers the cognitive (secondary) users (SUs) the ability to access the licensed spectrum in an opportunistic manner. More specifically,

Manuscript received November 6, 2013; revised February 20, 2014, April 21, 2014, June 10, 2014, and July 17, 2014; accepted July 18, 2014. Date of publication August 1, 2014; date of current version September 19, 2014. This paper was supported by NPRP under Grant 09-126-2-054 from the Qatar National Research Fund (a member of Qatar Foundation). The statements made herein are solely the responsibility of the authors. An earlier version of this work was presented at IEEE SPAWC, Darmstadt, Germany, June 2013 [18]. The associate editor coordinating the review of this paper and approving it for publication was Y. Chen.

A. Afana is with the Department of Electrical and Computer Engineering, Concordia University, Montreal, QC H3G 2W1, Canada (e-mail: a_afa@encs.concordia.ca).

A. Ghayeb is with the Department of Electrical and Computer Engineering, Texas A&M University at Qatar, Doha, Qatar, on leave from the Concordia University, Montreal, QC H4B 1R6, Canada (e-mail: ali.ghayeb@qatar.tamu.edu).

V. Asghari and S. Affes are with the Institut National de la Recherche Scientifique (INRS), University of Quebec, Montreal, QC H5A 1K6, Canada (e-mail: vahid@emt.inrs.ca; affes@emt.inrs.ca).

Color versions of one or more of the figures in this paper are available online at <http://ieeexplore.ieee.org>.

Digital Object Identifier 10.1109/TCOMM.2014.2345406

the cognitive radio techniques allow SUs to sense the unused spectrum (spectrum sensing), to manage the best available spectrum to fulfill the user communication demands (spectrum management), and to provide a fair spectrum sharing among all coexisting users (spectrum sharing) [1]. Two main approaches of spectrum sharing are identified in the literature [2]. One is the underlay approach which operates over ultra-wide frequency bands with strict restrictions on the transmitted power levels, and the other is the overlay approach, which is based on giving higher priority for primary users through the use of spectrum sensing and adaptive allocation. While the underlay approach allows multiple systems to be deployed in overlapping locations and spectrum, in the overlay approach, the CR users try to access the available spectrum without causing interference to the primary users (PUs). To meet this limitation, SUs adapt their transmit powers or make use of other degrees of freedom such as *beamforming* to ensure the quality-of-service (QoS) of the PU while enhancing their own performance [3].

Cooperative relaying emerged as a powerful solution for improving the performance of single-antenna communication nodes. This is gained by incorporating intermediate relay nodes, which are used to assist transmission from the source to the destination. There are two types of cooperative relaying networks according to the relaying directions known as one-way and two-way relaying. Two-way relaying achieves higher bandwidth efficiency than one-way relaying. Both techniques have been extensively studied in the traditional non-cognitive radio sense. The authors in [4]–[6] and references therein consider threshold-based relaying strategies for two-way decode-and-forward (DF) (digital network coding) cooperative communication networks in an effort to mitigate the impact of error propagation, resulting in preserving the diversity order of the system. In [7]–[12], two-way amplify-and-forward (AF) (analog network coding) cooperative relaying networks are investigated where the performance of two, three and four time-slot transmission protocols are compared and analyzed.

A common conclusion shared by all mentioned published papers is that the two time-slot (2-TS) transmission protocol offers an improved spectral efficiency as compared to the three time-slot (3-TS) transmission strategy. However, such conclusion ignores the fact that, for the 2-TS protocol, the number of degrees of freedom decreases, and at the same time, the level of interference at the relays increases. This motivates us to study the tradeoff between the two schemes in terms of bandwidth efficiency, relay power consumption, and interference cancellation in spectrum-sharing systems.

Applying the concept of cooperative relaying in spectrum-sharing systems has recently received considerable interest due

to its efficacy in guaranteeing reliable transmission for secondary systems [13], [14]. In [14], a dual-hop relaying system is studied, in which a secondary source wishes to send data to a destination employing either DF or AF relaying strategy in the presence of one PU. While cooperative one-way relaying systems in cognitive radio networks (CRNs) have been heavily studied, two-way relaying in spectrum-sharing environments received little attention [15], [16]. Recently, in [15], outage probability expressions for both primary and secondary systems were derived in a cooperative two-way DF relaying system where a SU helps two primary transceivers to communicate with each other. In [16], the outage performance of a two-way AF relaying system in a spectrum sharing environment was investigated. However, in [15] and [16], an overlay spectrum-sharing scenario is assumed.

Beamforming is an alternative emerging technology proposed to alleviate the inflicted interference in spectrum-sharing systems [17], [18]. Recently, applying beamforming in cooperative CRNs has received great interest [19]–[21]. For instance, in [19], an iterative alternating optimization-based algorithm was developed to obtain the optimal beamforming weights to maximize the worst signal-to-interference-noise (SINR) ratio. Convex optimization methods are used to optimize the beamforming weights in an overlay cognitive system [20]. However, these algorithms and tools suffer from high computational complexity. Zero forcing beamforming (ZFB) is a simple sub-optimal approach that can be practically implemented. In [21], a ZFB approach is applied to improve the primary system performance in an overlay CR scenario with multi-antenna system. However, all these works assume cooperative one-way relaying.

Recently, the problem of sum-rate maximization under constraints on interference on a primary receiver for multi-antenna cognitive two-way relay network has been investigated in [22]. In that paper, the authors have provided a structure of the optimal relay beamformer and proposed projection-based sub-optimal beamforming schemes such as zero-forcing reception-orthogonally projected zero-forcing transmission. The authors in [23] have obtained the optimal beamforming coefficients in a cognitive two-way relaying system using iterative semidefinite programming (SDP) and bisection search methods with the objective of minimizing the interference at the PU with SUs' SINR constraints. This scheme suffers from high computational complexity and implementation difficulties. We remark that all previous works considered only one primary user that coexists with the secondary users. Recently, in [24], the authors have proposed a transceiver design for an overlay cognitive two-way relay network where a secondary multi-antenna relay helps two PUs to communicate between themselves. Optimal precoders using SDP methods are found with the aim of maximizing the achievable transmission rate of the SU while maintaining the rate requirements of the PUs for different relay strategies.

Motivated by the great potential of combining two-way relaying and beamforming, we use in this paper collaborative distributed ZFB in two-way AF relaying in a spectrum sharing environment. In particular, we consider a spectrum-sharing system comprising two secondary sources communicating with each other in two or three consecutive time slots, a number of secondary AF relays and a number of PUs. The available relays

that receive the signals (from the sources) are used for relaying in the second time-slot or in the third time-slot according to the adopted transmission protocol. Specifically, the selected relays employ distributed ZFB to null the inflicted interference on the PUs in the relaying phase in addition to improve the performance of the secondary system. We also limit the interference from the secondary sources by imposing peak constraints on their transmit powers in the broadcasting phase. Based on the aforementioned facts, comparing the 2-TS and 3-TS-based distributed beamforming techniques in spectrum-sharing systems is important because the 3-TS protocol offers certain advantages, which can result in improved performance of two-way network beamforming as compared to the 2-TS protocol. These advantages include the additional degrees of freedom in suppressing the interference. While such a comparison may include the four time-slot protocol, in this paper, we restrict our investigation to the 2-TS and 3-TS protocols as these two competing protocols are more feasible among the two-way network beamforming techniques. To study and compare the performance tradeoffs between the two transmission protocols, we derive the cumulative distribution functions (CDF) and the moment generating function (MGF) of the end-to-end equivalent signal-to-noise ratio (SNR) in both protocols. Exploiting these statistics, the outage probability and the average error probability are derived. It is shown that the ZFB approach has the potential of improving the secondary performance and limiting the interference in a simple practical manner compared to other complex approaches.

Our main contributions and differences from other works can be summarized as follows:

- We derive closed-form expressions for the outage and average error probabilities for the two transmission protocols (2-TS and 3-TS) and confirm the results numerically as well as by simulations for different values of interference temperatures Q , different number of relays and different number of PUs.
- We derive the diversity order of the proposed system by analyzing the asymptotic behavior of the secondary system performance at high SNRs (high values of Q). We show that the diversity order is $(L_s - M)$ which indicates that the diversity order increases linearly with increasing the number of secondary relays L_s and decreasing the number of primary receivers M .
- The beamforming weights at the secondary relays are optimized to maximize the received SNR at the secondary receivers subject to nulling the interference inflicted on the existing primary users. From the closed-form solutions of the weight vectors, we propose a distributed scheme that requires little cooperation between the two transceivers and the relays, which leads to a reduced overhead.
- Compared to [23] where optimal beamforming weights are obtained via iterative and semidefinite relaxation methods, our proposed scheme exploits ZFB as a sub-optimal approach to obtain the beamforming weights using a standard linear optimization method. Moreover, we consider a more general assumption by considering multiple existing PUs where [23] considers only one PU.

- Comparison between the performances of the 2-TS and 3-TS based ZFB techniques is evaluated and discussed. It is demonstrated that the 3-TS protocol outperforms the 2-TS protocol in terms of performance in certain practical scenarios. We show that this occurs when the two transceivers transmit at different powers as the 3-TS scheme allocates more power to the received signal transmitted from the transceiver with a higher power. The advantage of the 2-TS scheme, however, is that it achieves higher bandwidth efficiency.
- Comparison between the sum-rate performances of the optimal beamforming scheme and the adopted sub-optimal ZFB scheme is simulated and discussed in the numerical results. It is demonstrated that the adopted sub-optimal scheme presents a good performance with less complexity and therefore offers a good compromise between complexity and performance.

The rest of this paper is organized as follows. Section II describes the system model. The transmission protocols are presented in Section III. ZFB weight design is described in Section IV. Section V introduces the end-to-end SNR analysis. The outage probability analysis of the 2-TS and 3-TS protocols is analyzed in Section VI while the average error probability analysis is analyzed in Section VII. Numerical results and discussions are given in Section VIII. Section IX concludes the paper.

Throughout this paper, the Frobenius norm of the vectors are denoted by $\|\cdot\|$. The Transpose and the Conjugate Transpose operations are denoted by $(\cdot)^T$ and $(\cdot)^\dagger$, respectively. $|x|$ means the magnitude of a complex number x . $\mathcal{CN}(0,1)$ refers to a complex Gaussian normal random variable with zero-mean and unit variance. $\text{Diag}(\mathbf{x})$ denotes a diagonal matrix whose diagonal elements are the elements of \mathbf{x} and $\text{Diag}(\mathbf{X})$ is a vector which contains the diagonal entries of the square matrix \mathbf{X} .

II. SYSTEM AND CHANNEL MODELS

We consider a two-way relaying system that is composed of two secondary transceivers S_j , $j = 1, 2$ and a set of L_s AF secondary relays denoted by R_i for $i = 1, \dots, L_s$ coexisting in the same spectrum band with M primary receivers (PUs) as shown in Fig. 1.¹ All nodes are equipped with one antenna. The two sources wish to communicate with each other in a half-duplex way. There is no direct link between the sources and thus they can only exchange messages via relay nodes. The SUs are allowed to share the same frequency spectrum with the PUs as long as the interference to the PUs is limited to a predefined threshold. Both systems transmit simultaneously in an underlay manner.

We consider in this work two transmission protocols, the first protocol is the 2-TS scheme, and the second protocol is the 3-TS scheme [7]. In 2-TS, in the first time-slot (TS₁), based on the interference channel state information (CSI) from S_1 to the p th PU, which suffers the most interference caused by

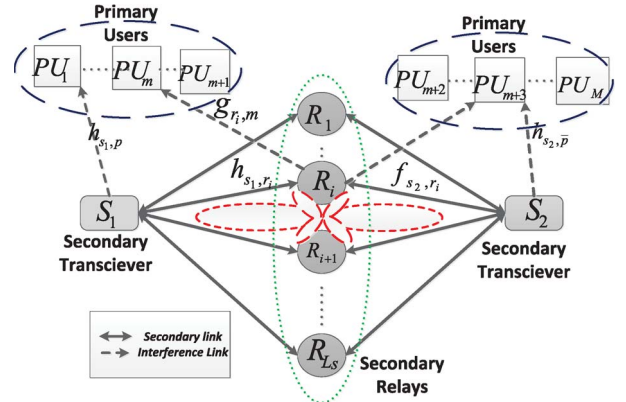


Fig. 1. Spectrum-sharing system with two-way AF relaying.

S_1 , S_1 adjusts its transmit power under predefined threshold Q_1 and broadcasts its message to all relays. Simultaneously, in TS₁, based on the interference CSI from S_2 to the \bar{p} th PU, which suffers the most interference caused by S_2 (the p th and \bar{p} th PUs could be different or the same), S_2 adjusts its transmit power under predefined threshold Q_2 and broadcasts its message to all relays.² In the second time-slot (TS₂), ZFB is applied to null the interference from the relays L_s (that are allowed to participate) to the PUs so that the relays are always able to transmit without interfering with the PUs. The ZFB processing vector, namely \mathbf{w}_{zf} , is optimized to maximize the received SNRs at both transceivers while nulling the inflicted interference to the existing PUs.

Similarly, in TS₁ of the 3-TS protocol, S_1 adjusts its transmit power under a predefined threshold Q_1 and broadcasts its message to all relays. In TS₂, S_2 also transmits its message to all relays under a tolerable threshold Q_2 . In the third time-slot (TS₃), ZFB is applied to null the interference from the L_s relays to the PUs. Two ZFB weight vectors, namely $\mathbf{w}_{\text{zf}1}$ and $\mathbf{w}_{\text{zf}2}$, are optimized so as to maximize the received SNRs at S_1 and S_2 , respectively, while nulling the inflicted interference to the existing PUs.

All channel coefficients are assumed to be independent Rayleigh flat fading and quasi-static, so that the channel gains remain unchanged during the transmission period. Let h_{s_1,r_i} , f_{s_2,r_i} denote the channel coefficients from the sources S_1 and S_2 to the i th relay, respectively, which are modeled as zero mean, circularly symmetric complex Gaussian (CSCG) random variables with variance λ_{s_1,r_i} , λ_{s_2,r_i} . Denote $h_{s_1,p}$ and $h_{s_2,\bar{p}}$ as the interference channel coefficients from S_1 and S_2 to the p th and \bar{p} th PUs, and their channel power gains are $|h_{s_1,p}|^2$ and $|h_{s_2,\bar{p}}|^2$, which are exponentially distributed with parameter $\lambda_{s_1,p}$ and $\lambda_{s_2,\bar{p}}$, respectively. Let the ZFB vector in the 2-TS protocol be $\mathbf{w}_{\text{zf}} = [w_1, w_2, \dots, w_{L_s}]$ where $\mathbf{W}_{\text{zf}} = \text{Diag}(\mathbf{w}_{\text{zf}})$. Also, let the ZFB vectors in the 3-TS protocol be $\mathbf{w}_{\text{zf}1}^T = [w_{11}, w_{12}, \dots, w_{1L_s}]$ used to direct the signal to S_1 and $\mathbf{w}_{\text{zf}2}^T = [w_{21}, w_{22}, \dots, w_{2L_s}]$ used to direct the signal to S_2 . Let $\mathbf{h}^T = [h_{r_1,s}, \dots, h_{r_{L_s},s}]$ and $\mathbf{f}^T = [f_{r_1,s}, \dots, f_{r_{L_s},s}]$ be the channel vectors between the relays

¹Hereafter, in the secondary system, we use the term “transceiver” instead of transmitter and receiver. Meanwhile, we use transmitter and receiver terms in the primary system.

²When the PUs are affected from the interference of both transceivers simultaneously, Q_1 and Q_2 could be optimized to maximize the SU performance such that QoS at the PUs is ensured.

and S_1 and S_2 , respectively. Let $\mathbf{G}_{\text{rp}}^T = [\mathbf{g}_{\text{r},\text{p}_1}, \dots, \mathbf{g}_{\text{r},\text{p}_M}]$ be the channel matrix between the relays and all M PUs where $\mathbf{g}_{\text{r},\text{p}_m} = [g_{r_1,\text{p}_m}, \dots, g_{r_{L_s},\text{p}_m}]$.

It is assumed that S_1 and S_2 have perfect knowledge of their interference channel power gains, which can be acquired through a spectrum-band manager that mediates between the primary and secondary users [1], [16], [21], [22], [26]–[29]. It is also assumed that the i th relay knows the CSI for the links $(R_i - S_j)$. In the underlying system model, full knowledge of the CSI \mathbf{h} and \mathbf{f} is assumed at S_1 and S_2 [10]. In practice, this CSI can be obtained by the traditional channel training, estimation, and feed-back mechanisms as in [25]. Also, the transceivers are assumed to have full knowledge of the interference between relays and PUs, i.e., \mathbf{G}_{rp} . We acknowledge that obtaining the interference might be a challenging problem in practice. To this end, several protocols have been proposed in [1], [26]–[29], which allow secondary and primary users to collaborate and exchange information such that the interference channel gains can be directly fed-back from the primary receiver to the secondary network. In practice, for a primary licensee that allows the secondary to access the spectrum band, presumably for a fee, certain cooperation between the primary and secondary networks can be expected [27]. Exploiting the knowledge of the CSI at the transceivers, \mathbf{w}_{zf_1} and \mathbf{w}_{zf_2} are designed at S_1 and S_2 and sent back to the relays by only one of the transceivers via low data-rate feedback links, and that is applicable in slow fading environments [11], [12]. We argue later that each relay (exploiting the knowledge of the CSI between itself and both transceivers) can calculate its own optimal beamforming weight based only on the information that are broadcasted to all relays by the two transceivers.³

III. TRANSMISSION PROTOCOLS

A. 2-TS Protocol

In this scheme, the sources communicate with each other over two time-slots. In the first time slot, S_1 and S_2 broadcast their signals to the relays simultaneously. The received signal at the i th relay in TS₁ can be written as

$$y_{r_i}^1 = \sqrt{P_1} h_{s_1,r_i} x_{s_1} + \sqrt{P_2} f_{s_2,r_i} x_{s_2} + n_1, \quad (1)$$

where P_1 and P_2 are the transmit powers of S_1 and S_2 , respectively, x_{s_1} and x_{s_2} are the information symbols of S_1 and S_2 with $\mathbb{E}[|x_{s_1}|^2] = \mathbb{E}[|x_{s_2}|^2] = 1$ and n_1 denotes the zero-mean CSCG noise at the i th relay with variance σ^2 in TS₁. In the second time slot, the relays weight the received signals

³It is also assumed that the interference from the primary transmitter is treated as additive white Gaussian noise (AWGN), which accounts for the worst case scenario, but leads to tractable upper-bounds on the performance of the secondary system [29], and is justified in the following cases: 1) the interference is represented in terms of AWGN when the primary transmitter's signal is generated by random Gaussian codebooks [28], [29]; and 2) as a practical scenario, consider a heterogeneous network in which the primary transmitter is a macro base station and the secondary transceiver could be a femto base station. When both base stations are far away from each other, which is mostly the case, they do not impose interference on each other [42]. It is worth noting that this assumption is widely used in the literature (see for example [16], [21], [29]).

and forward them to the two sources. The weighted transmitted signal in a vector form is

$$\mathbf{x}_{\text{R}} = \text{Diag}(\mathbf{w}_{\text{zf}}) \mathbf{y}_{\text{r}}^1, \quad (2)$$

where \mathbf{y}_{r}^1 is the relays received signals in a vector form. The received signal at S_2 is given as

$$y_{S_2}^2 = \sqrt{P_1} B_r \mathbf{f}^\dagger \text{Diag}(\mathbf{w}_{\text{zf}}) \mathbf{h} x_{s_1} + \sqrt{P_2} B_r \mathbf{f}^\dagger \text{Diag}(\mathbf{w}_{\text{zf}}) \mathbf{f} x_{s_2} + B_r \mathbf{f}^\dagger \text{Diag}(\mathbf{w}_{\text{zf}}) \mathbf{n}_1 + n_{s_2}, \quad (3)$$

where n_{s_2} denotes the zero-mean CSCG noise at S_2 with variance σ^2 , and B_r is the normalization constant designed to ensure that the total transmit power at the relays is constrained, and they are given as [7]

$$B_r = \sqrt{\frac{P_r}{P_1 \|\mathbf{W}_{\text{zf}} \mathbf{h}\|^2 + P_2 \|\mathbf{W}_{\text{zf}} \mathbf{f}\|^2 + \text{Trace}(\mathbf{W}_{\text{zf}} \mathbf{W}_{\text{zf}}^\dagger) \sigma^2}}, \quad (4)$$

where P_r is the total transmit power at the relays.

As the two transceivers have perfect knowledge of \mathbf{h} , \mathbf{f} and \mathbf{G}_{rp} [10], the transceivers can use this knowledge to determine the self-interference signal. Note that the second term in (3) depends on the signal transmitted by S_2 during the first time slot. Also, the weight vector \mathbf{w}_{zf} is calculated at this transceiver [11], [12]. Furthermore, B_r is known at both transceivers. Therefore, the second term in (3) is known at S_2 . Hence, this self-interference term can be removed and the received signal at S_2 becomes

$$y_{S_2}^2 = \sqrt{P_1} B_r \mathbf{f}^\dagger \text{Diag}(\mathbf{w}_{\text{zf}}) \mathbf{h} x_{s_1} + B_r \mathbf{f}^\dagger \text{Diag}(\mathbf{w}_{\text{zf}}) \mathbf{n}_1 + n_{s_2}. \quad (5)$$

The combined received SNR at S_2 in the 2-TS protocol is given as

$$\gamma_{eq}^{2\text{-TS}} = \frac{P_1 B_r^2 \|\mathbf{f}^\dagger \text{Diag}(\mathbf{z} \mathbf{w}_{\text{zf}}) \mathbf{h}\|^2}{B_r^2 \|\mathbf{f}^\dagger \text{Diag}(\mathbf{w}_{\text{zf}})\|^2 \sigma^2 + \sigma^2}. \quad (6)$$

Similarly, the total received SNR at S_1 is obtained with the notations interchanged. Hereafter, since the analysis is the same for S_1 and S_2 , we consider only S_2 .

B. 3-TS Protocol

As mentioned above, the communication process occurs over three time-slots. In TS₁, S_1 broadcasts its signal x_{s_1} to all relays, then the received signal at the i th relay is given as

$$y_{r_i}^1 = \sqrt{P_1} h_{s_1,r_i} x_{s_1} + n_1, \quad (7)$$

In TS₂, S_2 broadcasts its signal x_{s_2} to all relays, then the received signal at the i th relay is

$$y_{r_i}^2 = \sqrt{P_2} f_{s_2,r_i} x_{s_2} + n_2, \quad (8)$$

where n_2 denotes zero-mean CSCG noise at the i th relay with variance σ^2 during TS₂. In TS₃, the relays combine linearly the weighted received signals from TS₁ and TS₂ and forward the sum to both transceivers, e.g., the i th relay forwards

$(w_{i,2}y_{r_i}^1 + w_{i,1}y_{r_i}^2)$ to both S_1 and S_2 . As such the received signal at S_2 in a vector form

$$\begin{aligned} y_{S_2}^3 &= \sqrt{P_2}\bar{B}_r\sqrt{(1-\alpha)}\mathbf{f}^\dagger\text{Diag}(\mathbf{w}_{zf1})\mathbf{f}x_{s_2} \\ &+ \sqrt{P_1}\bar{B}_r\sqrt{\alpha}\mathbf{f}^\dagger\text{Diag}(\mathbf{w}_{zf2})\mathbf{h}x_{s_1} \\ &+ \bar{B}_r\sqrt{\alpha}\mathbf{f}^\dagger\text{Diag}(\mathbf{w}_{zf2})\mathbf{n}_1 \\ &+ \bar{B}_r\sqrt{(1-\alpha)}\mathbf{f}^\dagger\text{Diag}(\mathbf{w}_{zf1})\mathbf{n}_2 + n_{s_2}, \end{aligned} \quad (9)$$

where \bar{B}_r is the normalization constant designed to ensure that the total transmit power at the relays is constrained and they are given as [7]

$$\bar{B}_r = \sqrt{\frac{P_r}{Z}}, \quad (10)$$

where $Z = \text{Trace}((1-\alpha)(\mathbf{w}_{zf1}\mathbf{h}^\dagger\mathbf{h}\mathbf{w}_{zf1}^\dagger)) + \text{Trace}(\alpha(\mathbf{w}_{zf2}\mathbf{f}^\dagger\mathbf{f}\mathbf{w}_{zf2}^\dagger)) + \sigma^2$ and α is the power allocation parameter used to allocate the available power at the relays with $0 < \alpha < 1.4$. As S_1 and S_2 know the CSI and their transmitted signal, the self-interference term (first term) can be perfectly subtracted before further processing of the received signals. After removing the negligible noise term (fourth term), (9) reduces to⁵

$$\begin{aligned} y_{S_2}^3 &= \sqrt{P_1}\bar{B}_r\sqrt{\alpha}\mathbf{f}^\dagger\text{Diag}(\mathbf{w}_{zf2})\mathbf{h}x_{s_1} \\ &+ \bar{B}_r\sqrt{\alpha}\mathbf{f}^\dagger\text{Diag}(\mathbf{w}_{zf2})\mathbf{n}_2 + n_{s_2}. \end{aligned} \quad (11)$$

Then the total received SNR at S_2 in the 3-TS protocol is given as

$$\gamma_{eq}^{3\text{-TS}} = \frac{P_1\bar{B}_r^2\alpha\|\mathbf{f}^\dagger\text{Diag}(\mathbf{w}_{zf2})\mathbf{h}\|^2}{\bar{B}_r^2\alpha\|\mathbf{f}^\dagger\text{Diag}(\mathbf{w}_{zf2})\|^2\sigma^2 + \sigma^2}. \quad (12)$$

IV. ZFB WEIGHTS DESIGN

Our objective here is to maximize the received SNRs at the two transceivers to enhance the performance of the secondary system while limiting the interference reflected on the PUs. Due to its simplicity and low complexity, ZFB is applied as an alternative to the optimal scheme. To be able to apply ZFB, the general assumption that the number of relays must be greater than the number of primary receivers is considered, hence, $L_s > M$.

A. 2-TS Protocol

In this subsection, we derive the ZFB vector \mathbf{w}_{zf} in the 2-TS protocol. As we use a suboptimal approach, we first derive the two beamforming vectors \mathbf{w}_{zf1} and \mathbf{w}_{zf2} that are designed to direct the desired signals to S_1 and S_2 , respectively. Then we combine them in a one beamforming vector as will be shown below.

⁴ α is chosen to satisfy the minimum average error probability at the two secondary transceivers. Since the optimization problem is very complicated to get an optimal solution in closed-form, it can be solved numerically. When α is optimized, the secondary system performance should perform better than when it is fixed (more details in the Section VII).

⁵ \mathbf{w}_{zf1} is designed to direct the signal to S_1 as will be explained in the next section. The term $\|\mathbf{f}^\dagger\text{Diag}(\mathbf{w}_{zf1})\|^2$ results in a negligible gain. This is verified through simulations.

According to the ZFB principles, the transmit weight vectors \mathbf{w}_{zf1} , \mathbf{w}_{zf2} are chosen to lie in the orthogonal space of \mathbf{G}_{rp}^\dagger such that $|\mathbf{g}_{r,p_i}^\dagger\mathbf{w}_{zf1}| = 0$ and $|\mathbf{g}_{r,p_i}^\dagger\mathbf{w}_{zf2}| = 0$, $\forall i = 1, \dots, M$ and $|\mathbf{h}^\dagger\mathbf{w}_{zf1}|$, $|\mathbf{f}^\dagger\mathbf{w}_{zf2}|$ are maximized. So the problem formulation for finding the optimal weight vectors is divided into two parts as follows.

$$\begin{aligned} \max_{\mathbf{w}_{zf1}} \quad & |\mathbf{h}^\dagger\mathbf{w}_{zf1}| \\ \text{s.t.} \quad & |\mathbf{g}_{r,p_i}^\dagger\mathbf{w}_{zf1}| = 0, \quad \forall i = 1, \dots, M \quad \|\mathbf{w}_{zf1}\| = 1. \end{aligned} \quad (13)$$

$$\begin{aligned} \max_{\mathbf{w}_{zf2}} \quad & |\mathbf{f}^\dagger\mathbf{w}_{zf2}| \\ \text{s.t.} \quad & |\mathbf{g}_{r,p_i}^\dagger\mathbf{w}_{zf2}| = 0, \quad \forall i = 1, \dots, M \quad \|\mathbf{w}_{zf2}\| = 1. \end{aligned} \quad (14)$$

By applying a standard Lagrangian multiplier method, the weight vectors that satisfy the above optimization methods are given as

$$\mathbf{w}_{zf1} = \frac{\Xi^\perp\mathbf{h}}{\|\Xi^\perp\mathbf{h}\|}, \quad (15)$$

and

$$\mathbf{w}_{zf2} = \frac{\Xi^\perp\mathbf{f}}{\|\Xi^\perp\mathbf{f}\|}, \quad (16)$$

where $\Xi^\perp = (\mathbf{I} - \mathbf{G}_{rp}(\mathbf{G}_{rp}^\dagger\mathbf{G}_{rp})^{-1}\mathbf{G}_{rp}^\dagger)$ is the projection idempotent matrix with rank $(L_s - M)$. The rank of the matrix is approved from the following Lemma in the projection matrix theory [30].

Lemma 1: Let \mathbf{G} be an $n \times k$ matrix with full column rank k , $k < n$, then the nonzero matrix $\mathbf{G}(\mathbf{G}^\dagger\mathbf{G})^{-1}\mathbf{G}^\dagger$ is an idempotent symmetric matrix and its orthogonal projection matrix is $\mathbf{I} - \mathbf{G}(\mathbf{G}^\dagger\mathbf{G})^{-1}\mathbf{G}^\dagger$ with rank $(n - k)$ [30, Theorems 4.21, 4.22].

It can be observed from the rank of the matrix that the cooperative ZFB beamformer becomes effective only when $L_s > M$. Otherwise, the interference from secondary relays to primary receivers cannot be mitigated. The case when $L_s \leq M$ can be handled using conventional schemes by limiting the interference via transmit power control methods, e.g., [15], [16].

In the 2-TS protocol, since each relay knows the CSI of the channels between itself and both secondary sources and between itself and the primary receivers, the ZFB matrix \mathbf{w}_{zf} is made up by the diagonal of the product of the two ZFB vectors \mathbf{w}_{zf1} (used to direct the signal to S_1) and \mathbf{w}_{zf2} (used to direct the signal to S_2) which is represented as [8], [9] and references therein

$$\mathbf{w}_{zf} = \text{Diag}(\mathbf{w}_{zf1}\mathbf{w}_{zf2}^T). \quad (17)$$

Proof: Let $\mathbf{H}_{UL} = [\mathbf{h}, \mathbf{f}]$ with dimension space $L_s \times 2$, and $\mathbf{H}_{DL} = [\mathbf{f}, \mathbf{h}]^T$ with dimension space $2 \times L_s$. First, construct the subspace Ξ^\perp such as $\Xi^\perp = (\mathbf{I} - \mathbf{G}_{rp}(\mathbf{G}_{rp}^\dagger\mathbf{G}_{rp})^{-1}\mathbf{G}_{rp}^\dagger)$ with $L_s \times L_s$ dimension. Second, project the CR channels to the space Ξ^\perp , utilizing that Ξ^\perp is idempotent matrix, i.e., $\Xi^\perp = (\Xi^\perp)^2$, then $\mathbf{H}_{DL}\Xi^\perp\mathbf{H}_{UL} = \mathbf{H}_{DL}\Xi^\perp\Xi^\perp\mathbf{H}_{UL}$. Third, perform ZFB to the CRs within the subspace orthogonal to the PU channel with the power constraint $\mathbf{W}_{zf} =$

$(\mathbf{H}_{\text{DL}}\mathbf{\Xi}^\perp)^T \begin{bmatrix} \frac{1}{\|\mathbf{\Xi}^\perp \mathbf{h}\|} & 0 \\ 0 & \frac{1}{\|\mathbf{\Xi}^\perp \mathbf{f}\|} \end{bmatrix} (\mathbf{\Xi}^\perp \mathbf{H}_{\text{UL}})^T$. This results in $\mathbf{W}_{\text{zf}} = \text{Diag}(\mathbf{w}_{\text{zf}_1} \mathbf{w}_{\text{zf}_2}^T)$. \square

It is worth noting that the weight matrix is diagonal, which guarantees that the relays transmit only their own received signal and there is no data exchange among the relays. Thus, the algorithm works in a distributed manner.

B. 3-TS Protocol

The ZFB vectors in 3-TS protocol are simply chosen to be \mathbf{w}_{zf_1} and \mathbf{w}_{zf_2} given by (15) and (16) in the first and second time-slot, respectively. In the third time-slot, the weighted received signals are combined linearly with certain power allocation values as described previously.

Remark: By having a closer look at the closed-form solutions of the optimal weight vectors in (15) and (16), we propose a distributed implementation instead of the centralized one mentioned before. From (15) and (16), to design \mathbf{w}_{zf_1} and \mathbf{w}_{zf_2} at the relays, each relay needs the global constants $(1/\|\mathbf{\Xi}^\perp \mathbf{h}\|)$ and $(1/\|\mathbf{\Xi}^\perp \mathbf{f}\|)$ and also the interference matrix, i.e. $\mathbf{\Xi}^\perp$, which are broadcasted by either S_1 or S_2 . Upon receiving the broadcast messages from S_1 or S_2 , each i th relay node determines the optimal w_{1i} and w_{2i} weights from its local information of h_{r_i, s_1} and f_{r_i, s_2} . As such, the beamforming computation is calculated in a distributed manner.

V. END-TO-END SNR ANALYSIS

A. First Order Statistics of $\gamma_{eq}^{2\text{-TS}}$

In the underlay approach of this model, the secondary source can utilize the PU's spectrum as long as the interference it generates at the PUs remains below the interference threshold Q_j , $\forall j = 1, 2$. For that reason, P_j is constrained as $P_j = \min\{(Q_j/|h_{s_j, p}|^2), P_{s_j}\}$ where P_{s_j} is the maximum transmission power of S_j [18]. So the received SNR γ_{s_j, r_i} at the i th relay is given as

$$\gamma_{s_j, r_i} = \begin{cases} \frac{P_{s_j} |f_{s_j, r_i}|^2}{\sigma^2}, & P_{s_j} < \frac{Q_j}{|h_{s_j, p}|^2} \\ \frac{Q_j |f_{s_j, r_i}|^2}{\sigma^2 |h_{s_j, p}|^2}, & P_{s_j} \geq \frac{Q_j}{|h_{s_j, p}|^2} \end{cases}, \quad (18)$$

where σ^2 is the noise variance at each relay. We focus on the analysis of the second case ($P_{s_j} \geq (Q_j/|h_{s_j, p}|^2)$) as it is more effective and restrictive than the first case ($P_{s_j} < (Q_j/|h_{s_j, p}|^2)$). It determines the effect of the peak power constraint in the first time-slot on the performance of the secondary system while the system in the first case becomes a non-cognitive system. So the transmit powers P_1 and P_2 are constrained as $P_1 \leq Q_1/|h_{s_1, p}|^2$ and $P_2 \leq Q_2/|h_{s_2, p}|^2$.

Substituting (4), and (17) into (6), and after simple manipulations, the equivalent SNR at S_2 can be written in the general form of $\gamma_{eq}^{2\text{-TS}} = \gamma_{1,2\text{TS}} \gamma_{3,2\text{TS}} / (\gamma_{1,2\text{TS}} + \gamma_{2,2\text{TS}} + \gamma_{3,2\text{TS}} + 1)$ as:

$$\gamma_{eq}^{2\text{-TS}} = \frac{\frac{P_1}{\sigma^2} \|\mathbf{\Xi}^\perp \mathbf{h}\|^2 \frac{P_2}{\sigma^2} \|\mathbf{\Xi}^\perp \mathbf{f}\|^2}{\frac{P_1}{\sigma^2} \|\mathbf{\Xi}^\perp \mathbf{h}\|^2 + \frac{P_2}{\sigma^2} \|\mathbf{\Xi}^\perp \mathbf{f}\|^2 + \frac{P_r}{\sigma^2} \|\mathbf{\Xi}^\perp \mathbf{f}\|^2 + 1}. \quad (19)$$

Considering the peak constraint on the received power at the most affected primary user, we substitute P_1 and P_2 into (19). Then $\gamma_{eq}^{2\text{-TS}}$ becomes

$$\gamma_{eq}^{2\text{-TS}} = \frac{\gamma_{q_1} \frac{\|\mathbf{\Xi}^\perp \mathbf{h}\|^2}{|h_{s_1, p}|^2} \gamma_r \|\mathbf{\Xi}^\perp \mathbf{f}\|^2}{\gamma_{q_1} \frac{\|\mathbf{\Xi}^\perp \mathbf{h}\|^2}{|h_{s_1, p}|^2} + \gamma_{q_2} \frac{\|\mathbf{\Xi}^\perp \mathbf{f}\|^2}{|h_{s_2, p}|^2} + \gamma_r \|\mathbf{\Xi}^\perp \mathbf{f}\|^2 + 1}, \quad (20)$$

where $\gamma_r = P_r/\sigma^2$, $\gamma_{q_1} = Q_1/\sigma^2$ and $\gamma_{q_2} = Q_2/\sigma^2$.

We first find the statistics of the new random variables defined above. Then, we compute the CDF and MGF of $\gamma_{eq}^{2\text{-TS}}$, which will be used in the derivation of the performance metrics. To continue, let $\gamma_{1,2\text{TS}} = \gamma_{q_1} (\|\mathbf{\Xi}^\perp \mathbf{h}\|^2/|h_{s_1, p}|^2)$, $\gamma_{2,2\text{TS}} = \gamma_{q_2} (\|\mathbf{\Xi}^\perp \mathbf{f}\|^2/|h_{s_2, p}|^2)$ and $\gamma_{3,2\text{TS}} = \gamma_r \|\mathbf{\Xi}^\perp \mathbf{f}\|^2$.

Lemma 2 (PDFs of $\gamma_{1,2\text{TS}}$ and $\gamma_{2,2\text{TS}}$): Let each entry of \mathbf{h} and \mathbf{f} be i.i.d. $\sim \mathcal{CN}(0, 1)$, then $\|\mathbf{\Xi}^\perp \mathbf{h}\|^2$ and $\|\mathbf{\Xi}^\perp \mathbf{f}\|^2$ are chi squared random variables with $2(L_s - M)$ degrees of freedom. Given that $|h_{s_1, p}|^2$ and $|h_{s_2, p}|^2$ are exponential random variables, the PDFs of $f_{\gamma_{1,2\text{TS}}}(\gamma)$ and $f_{\gamma_{2,2\text{TS}}}(\gamma)$ are given respectively by [13]:

$$f_{\gamma_{i,2\text{TS}}}(\gamma) = \frac{\lambda_{s_i, p} (L_s - M + 1) \gamma^{L_s - M}}{\gamma_{q_i}^{L_s - M} \left(\frac{\gamma}{\gamma_{q_i}} + \lambda_{s_i, p} \right)^{L_s - M + 2}}, \quad \forall i = 1, 2. \quad (21)$$

Lemma 3 (CDF of $\gamma_{3,2\text{TS}}$): Let each entry of \mathbf{f} be i.i.d. $\sim \mathcal{CN}(0, 1)$, then $\|\mathbf{\Xi}^\perp \mathbf{f}\|^2$ is a chi squared random variable with $2(L_s - M)$ degrees of freedom [31, Theorem 2 Ch.1]. The CDF of $\gamma_{3,2\text{TS}}$ can be expressed as

$$F_{\gamma_{3,2\text{TS}}}(\gamma) = 1 - \frac{\Gamma(L_s - M, \frac{\gamma}{\gamma_r})}{(L_s - M - 1)!}, \quad \gamma \geq 0. \quad (22)$$

B. First Order Statistics of $\gamma_{eq}^{3\text{-TS}}$

Substituting (10), (15) and (16) into (12), and after simple manipulations, the equivalent SNR at S_2 can be written in the general form of $\gamma_{eq}^{3\text{-TS}} = \gamma_{1,3\text{TS}} \gamma_{3,3\text{TS}} / (\gamma_{1,3\text{TS}} + \gamma_{2,3\text{TS}} + \gamma_{3,3\text{TS}} + 1)$ as:

$$\gamma_{eq}^{3\text{-TS}} = \frac{\frac{P_1}{\sigma^2} \|\mathbf{h}\|^2 \alpha \frac{P_2}{\sigma^2} \|\mathbf{\Xi}^\perp \mathbf{f}\|^2}{\frac{P_1}{\sigma^2} \|\mathbf{h}\|^2 + \frac{P_2}{\sigma^2} \|\mathbf{f}\|^2 + \alpha \frac{P_r}{\sigma^2} \|\mathbf{\Xi}^\perp \mathbf{f}\|^2 + 1}. \quad (23)$$

Again, considering the peak constraint on the received power at the most affected primary user, $\gamma_{eq}^{3\text{-TS}}$ becomes

$$\gamma_{eq}^{3\text{-TS}} = \frac{\gamma_{q_1} \frac{\|\mathbf{h}\|^2}{|h_{s_1, p}|^2} \gamma_{r_1} \|\mathbf{\Xi}^\perp \mathbf{f}\|^2}{\gamma_{q_1} \frac{\|\mathbf{h}\|^2}{|h_{s_1, p}|^2} + \gamma_{q_2} \frac{\|\mathbf{f}\|^2}{|h_{s_2, p}|^2} + \gamma_{r_1} \|\mathbf{\Xi}^\perp \mathbf{f}\|^2 + 1}, \quad (24)$$

where $\gamma_{r_1} = \alpha P_r/\sigma^2$.

Remark: We notice in (23) that the 3-TS protocol results in a different received SNRs at S_1 and S_2 , depending on the power allocation parameter α . However, for the 2-TS protocol, equal power allocation is used since the sum of the two signals at the relay(s) is weighted by the same vector. This gives an advantage to the 3-TS protocol since it benefits from allocating different transmit powers to the sources.

To proceed, let $\gamma_{1,3TS} = \gamma_{q_1}(\|\mathbf{h}\|^2/|h_{s_1,p}|^2)$, $\gamma_{2,3TS} = \gamma_{q_2}(\|\mathbf{f}\|^2/|h_{s_2,p}|^2)$ and $\gamma_{3,3TS} = \gamma_{r_1}\|\Xi^\perp \mathbf{f}\|^2$.

Lemma 3 (PDFs of $\gamma_{1,3TS}$ and $\gamma_{2,3TS}$): Let each entry of \mathbf{h} and \mathbf{f} be i.i.d. $\mathcal{CN}(0,1)$, then $\|\mathbf{h}\|^2$ and $\|\mathbf{f}\|^2$ are chi squared random variables with $2L_s$ degrees of freedom, Given that $|h_{s_1,p}|^2$ and $|h_{s_2,p}|^2$ are exponential random variables, the PDFs of $f_{\gamma_{1,3TS}}(\gamma)$ and $f_{\gamma_{2,3TS}}(\gamma)$ are given respectively by [13]:

$$f_{\gamma_{i,3TS}}(\gamma) = \frac{\lambda_{s_i,p} L_s (\gamma)^{L_s-1}}{(\gamma_{q_i})^{L_s} \left(\frac{\gamma}{\gamma_{q_i}} + \lambda_{s_i,p} \right)^{L_s+1}}, \quad i = 1, 2. \quad (25)$$

According to Lemma 3, the CDF of $\gamma_{3,3TS}$ is

$$F_{\gamma_{3,3TS}}(\gamma) = 1 - \frac{\Gamma\left(L_s - M, \frac{\gamma}{\gamma_{r_1}}\right)}{(L_s - M - 1)!}, \quad \gamma \geq 0. \quad (26)$$

In the subsequent sections, we consider the statistics of the random variable γ_{eq}^{iTS} defined by $\gamma_{eq}^{iTS} = (\gamma_{1,iTS} \gamma_{3,iTS} / (\gamma_{1,iTS} + \gamma_{2,iTS} + \gamma_{3,iTS}))$, $i = 2, 3$, which can be considered as a tractable tight upper bound to the actual equivalent SNR.

VI. OUTAGE PROBABILITY ANALYSIS

In this section, we derive the outage probability for both 2-TS and 3-TS. As previously mentioned, the interference CSI between S_1 and the p th PU, i.e., $h_{s_1,p}$ is unknown at S_2 , and $h_{s_2,p}$ is also unknown at S_1 . Due to this randomness, the end-to-end received SNR at each transceiver in (22) and (26) is still a random variable and there is no guarantee of zero-outage.

A. 2-TS Protocol

An outage event occurs when γ_{eq}^{2-TS} falls below a certain threshold γ_{th} , which can be characterized mathematically as follows.

$$P_{out}^{2-TS} = \Pr(\gamma_{eq}^{2-TS} < \gamma_{th}) = F_{\gamma_{eq}^{2-TS}}(\gamma_{th}). \quad (27)$$

Theorem 1: A closed-form expression for the outage probability in the 2-TS protocol for a two-way AF relaying in spectrum-sharing system is given by

$$\begin{aligned} P_{out}^{2-TS} = & 1 - \hat{b} \sum_{m=0}^{L_s-M-1} \sum_{k=0}^m \sum_{r=0}^k \frac{(\gamma_{th})^{k-r}}{m!} \binom{m}{k} \binom{k}{r} \hat{a}^{\frac{r}{2}} \\ & \times e^{-\frac{\gamma_{th}}{\gamma_r}} \frac{2^{-\frac{2L_s+2M-2-r}{2}}}{\sqrt{2\pi}} \sqrt{\frac{\hat{a}\gamma_{th}}{\gamma_r}} \left(\frac{\gamma_{th}}{\gamma_r}\right)^{m-\frac{3r}{2}} \\ & \times \sum_{p=0}^{L_s-M} \binom{L_s-M}{p} \gamma_{th}^{L_s-M-p} \sum_{s=0}^N \frac{1}{s!} \\ & \times \left(\frac{-\gamma_{th}^2}{\gamma_r} + \frac{\gamma_{th}\hat{a}}{\gamma_r} \right)^s \frac{2^{L_s-M+1}(\gamma_{th}+a)^\mu}{2\pi\Gamma(L_s-M+2)} \\ & \times G_{6,4}^{2,6} \left(\frac{4\gamma_r^2(\gamma_{th}+\hat{a})^2}{(\hat{a}\gamma_{th})^2} \middle| \begin{matrix} \Delta(2,1-\alpha_o), \Delta(1,1-b_r) \\ \Delta(2,(L_s+1)-\alpha_o), \Delta(1,1-a_r) \end{matrix} \right), \end{aligned} \quad (28)$$

where $\hat{a} = \lambda_{s_2,p}\gamma_{q_2}$, $\hat{b} = (L_s - M + 1)\Gamma(r + L_s - M + 1)$, $a_r = ((1/4) - (1/4)(-2L_s + 2M - 2 - r))$, $(3/4) - (1/4)$

$(-2L_s + 2M - 2 - r)$, $b_r = ((1/2) + (1/4)(1 - r))$, $(1/2) - (1/4)(1 - r)$, $(1/4)(1 - r)$, $(-1/4)(1 - r)$, $\mu_o = p - k + (3r/2) - s - L_s + M - 3/2$, $\alpha_o = \mu_o + L_s - M + 2$, $\Delta(i, a) = (a/i), (a + 1/i), \dots, (a - i + 1/i)$ and $G_{\cdot;\cdot}(\cdot|\cdot)$ is the Meijer's G-function defined in [34].

Proof: To derive the outage probability of γ_{eq}^{2-TS} , conditioned on $\gamma_{1,2TS}$ and $\gamma_{2,2TS}$, we first express the CDF of γ_{eq}^{2-TS} as

$$\begin{aligned} F_{\gamma_{eq}^{2-TS}}(\gamma_{th}) = & \int_0^\infty \Pr\left(\gamma_{3,2TS} < \frac{\gamma_{th}(y+z)}{y-\gamma_{th}}\right) \\ & \times f_{\gamma_{1,2TS}}(y) f_{\gamma_{2,2TS}}(z) dy dz. \end{aligned} \quad (29)$$

Using variable change, $w = y - \gamma_{th}$, and after some algebraic manipulations, we have

$$\begin{aligned} F_{\gamma_{eq}^{2-TS}}(\gamma_{th}) = & 1 - \int_0^\infty \Pr\left(\gamma_{3,2TS} \geq \frac{\gamma_{th}(w+\gamma_{th}+z)}{w}\right) \\ & \times f_{\gamma_{1,2TS}}(w+\gamma_{th}) f_{\gamma_{2,2TS}}(z) dw dz. \end{aligned} \quad (30)$$

Substituting in the complementary of the CDF of $\gamma_{3,2TS}$ and the PDF of $\gamma_{1,2TS}$ from (22) and (21), respectively, we obtain

$$\bar{F}_{\gamma_{3,2TS}}(\gamma) = \frac{1}{(L_s - M - 1)!} \Gamma\left(L_s - M, \frac{\gamma_{th}(w+\gamma_{th}+z)}{\gamma_r w}\right), \quad (31)$$

where $\bar{F}_{\gamma_{3,2TS}}(\gamma)$ denotes the complementary of the CDF of $\gamma_{3,2TS}$. Before proceeding in the derivation, (31) is expressed in another mathematical form using [34, eq. 8.352.2] and [34, eq. 1.111] as follows.

$$\begin{aligned} \bar{F}_{\gamma_{3,2TS}}(\gamma) = & e^{-\frac{\gamma_{th}(w+\gamma_{th}+z)}{\gamma_r w}} \sum_{m=0}^{L_s-M-1} \sum_{k=0}^m \sum_{r=0}^k \frac{1}{m!} \binom{m}{k} \\ & \times \binom{k}{r} \left(\frac{\gamma_{th}}{\gamma_r}\right)^{m-k+r} \left(\frac{\gamma_{th}^2}{w\gamma_r}\right)^{k-r} \left(\frac{z}{w}\right)^r. \end{aligned} \quad (32)$$

Then substituting (32) into (30) and after some mathematical manipulations, we have

$$\begin{aligned} F_{\gamma_{eq}^{2-TS}}(\gamma_{th}) = & 1 - \sum_{m=0}^{L_s-M-1} \sum_{k=0}^m \sum_{r=0}^k \frac{1}{m!} \left(\frac{\gamma_{th}}{\gamma_r}\right)^{m-k} \binom{m}{k} \\ & \times \binom{k}{r} e^{-\frac{\gamma_{th}}{\gamma_r}} \int_0^\infty \left(\frac{\gamma_{th}^2}{w\gamma_r}\right)^{k-r} f_{\gamma_{1,2TS}}(w+\gamma_{th}) \\ & \times \underbrace{\left(\int_0^\infty \left(\frac{\gamma_{th}z}{w\gamma_r}\right)^r e^{-\frac{z\gamma_{th}}{w\gamma_r}} f_{\gamma_{2,2TS}}(z) dz \right)}_{I_1} dw. \end{aligned} \quad (33)$$

The inner integral I_1 can be solved using the variable change, $u = z + \lambda_{s_2,p}\gamma_{q_2}$, leading to

$$I_1 = \int_{\lambda_{s_2,p}\gamma_{q_2}}^\infty \hat{a} L_s \left(\frac{\gamma_{th}}{w\gamma_r}\right)^r e^{-\frac{\gamma_{th}}{w\gamma_r}(u-\hat{a})} \frac{(u-\hat{a})^{r+L_s-M}}{(u)^{L_s-M+2}} du, \quad (34)$$

Using [34, eq. 3.383.4], I_1 results in

$$I_1 = \hat{a}^{\frac{r}{2}} \hat{b} \left(\frac{\gamma_{th}}{w\gamma_r} \right)^{-r/2} e^{\frac{\hat{a}\gamma_{th}}{2w\gamma_r}} W_{-\frac{2L_s+2M-2-r}{2}, \frac{1-r}{2}} \left(\frac{\hat{a}\gamma_{th}}{w\gamma_r} \right), \quad (35)$$

where $W_{\dots}(\cdot)$ is the Whittaker function [34]. Returning to the main expression in (33), after substituting the results in (35) with further simplifications, we obtain

$$\begin{aligned} F_{\gamma_{eq}^{2-TS}}(\gamma_{th}) &= 1 - \sum_{m=0}^{L_s-M-1} \sum_{k=0}^m \sum_{r=0}^k \frac{(\gamma_{th})^{k-r}}{m!} \binom{m}{k} \binom{k}{r} \hat{b} \\ &\times e^{-\frac{\gamma_{th}}{\gamma_r}} \left(\frac{\gamma_{th}}{\gamma_{r_1}} \right)^{m-\frac{3r}{2}} \hat{a}^{\frac{r}{2}} \\ &\times \int_0^\infty \left(\frac{1}{w} \right)^{k-\frac{3r}{2}} e^{-\frac{\gamma_{th}}{w\gamma_r} + \frac{\hat{a}\gamma_{th}}{2w\gamma_r}} \\ &\times W_{-\frac{2L_s+2M-2-r}{2}, \frac{1-r}{2}} \left(\frac{\hat{a}\gamma_{th}}{w\gamma_r} \right) \\ &\times f_{\gamma_{1,2TS}}(w + \gamma_{th}) dw. \end{aligned} \quad (36)$$

To the best of our knowledge, the integral I_2 in (36) has no closed-form solution. To solve I_2 , we first represent the exponential term using Taylor series representation [34, eq. 1.211.1], apply the binomial theorem [34, eq. 1.11.1] for the term $(w + \gamma_{th})^{L_s-M}$ and express the Whittaker function in terms of Meijer's G-function using [34, eq. 9.34.9] and [34, eq. 9.31.2], which after many manipulations results in

$$\begin{aligned} F_{\gamma_{eq}^{2-TS}}(\gamma_{th}) &= 1 - \sum_{m=0}^{L_s-M-1} \sum_{k=0}^m \sum_{r=0}^k \frac{(\gamma_{th})^{k-r}}{m!} \binom{m}{k} \binom{k}{r} \\ &\times \hat{b} \hat{a}^{\frac{r}{2}} e^{-\frac{\gamma_{th}}{\gamma_r}} \frac{2^{-\frac{2L_s+2M-2-r}{2}}}{\sqrt{2\pi}} \left(\frac{\gamma_{th}}{\gamma_r} \right)^{m-\frac{3r}{2}} \\ &\times \sqrt{\frac{\hat{a}\gamma_{th}}{\gamma_r}} \sum_{p=0}^{L_s-M} \binom{L_s-M}{p} \gamma_{th}^{L_s-M-p} \sum_{s=0}^N \frac{1}{s!} \\ &\times \left(\frac{-\gamma_{th}^2}{\gamma_r} + \frac{\gamma_{th}\hat{a}}{\gamma_r} \right)^s \\ &\times \int_0^\infty \left(\frac{w^{p-k+\frac{3r}{2}-s-1/2}}{(w + \gamma_{th} + \hat{a})^{L_s-M+2}} \right. \\ &\times \left. \left(G_{4,2}^{0,4} \left(\frac{4\gamma_r^2 w^2}{(\hat{a}\gamma_{th})^2} \middle| \begin{matrix} 1-b_r \\ 1-a_r \end{matrix} \right) \right) \right) dw. \end{aligned} \quad (37)$$

The integral in (37) is solved using [36, eq. 2.24.2.4, vol. 3], then after few simplifications, the outage probability in the 2-TS protocol is expressed as in (28), thus completing the proof. \square

We remark that the Taylor series in the outage expression is expressed in the form of a finite sum where only six terms are needed in the summation over index s to obtain the accuracy to the degree of seven decimals as will be explained in the numerical results. It is worth noting that the Meijer G-functions are easily implemented in many mathematical softwares such as **Mathematica** and **Matlab**.

B. 3-TS Protocol

Similarly, for this scheme, an outage event occurs when γ_{eq}^{3-TS} falls below a certain threshold γ_{th} . As such, P_{out}^{3-TS} can be expressed as

$$P_{out}^{3-TS} = \Pr(\gamma_{eq}^{3-TS} < \gamma_{th}) = F_{\gamma_{eq}^{3-TS}}(\gamma_{th}). \quad (38)$$

Theorem 2: A closed-form expression for the outage probability in the 3-TS protocol for a two-way AF relaying based distributed ZFB in spectrum-sharing system is given by

$$\begin{aligned} P_{out}^{3-TS} &= 1 - b \sum_{m=0}^{L_s-M-1} \sum_{k=0}^m \sum_{r=0}^k \frac{(\gamma_{th})^{k-r}}{m!} \binom{m}{k} \binom{k}{r} a^{\frac{r+1}{2}} \\ &\times e^{-\frac{\gamma_{th}}{\gamma_{r_1}}} \frac{2^{-\frac{2L_s-r}{2}}}{\sqrt{2\pi}} \left(\frac{\gamma_{th}}{\gamma_{r_1}} \right)^{m-\frac{3r+1}{2}} \\ &\times \sum_{p=0}^{L_s-1} \binom{L_s-1}{p} \gamma_{th}^{L_s-1-p} \sum_{s=0}^N \frac{1}{s!} \left(\frac{-\gamma_{th}^2 + \gamma_{th}a}{\gamma_{r_1}} \right)^s \\ &\times \frac{2^{L_s}(\gamma_{th} + a)^{\mu_1}}{2\pi\Gamma(L_s + 1)} \\ &\times G_{6,4}^{2,6} \left(\frac{4\gamma_{r_1}^2(\gamma_{th} + a)^2}{(a\gamma_{th})^2} \middle| \begin{matrix} \Delta(2,1-\alpha_1), \Delta(1,1-b_{r_1}) \\ \Delta(2,(L_s+1)-\alpha_1), \Delta(1,1-a_{r_1}) \end{matrix} \right), \end{aligned} \quad (39)$$

where $\mu_1 = p - k + (3r/2) - s - L_s - (1/2)$ and $\alpha_1 = \mu_1 + L_s + 1$, $a_{r_1} = ((1/4) - (1/4)(-2L_s - r))$, $(3/4) - (1/4)(-2L_s - r)$, $b_{r_1} = ((1/2) + (1/4)(1 - r))$, $(1/2) - (1/4)(1 - r)$, $(1/4)(1 - r)$, $(-1/4)(1 - r)$.

Proof: To derive the outage probability expression in the 3-TS protocol, we follow the same steps as performed in the case of the 2-TS protocol. This yields the expression in (40). Although we have multiple summations, all of them are finite and easy to compute numerically. \square

C. Asymptotic Outage Probability

Although the expressions in (28) and (40) enable numerical evaluation of the exact system outage performance, they do not provide useful insights on the effect of key parameters (e.g., the number of secondary relays, the number of PUs, etc.) that influence the system performance. To get more insights, we now introduce asymptotic outage probability expressions, i.e., $\gamma_{q_i} \rightarrow \infty$, for the 2-TS and 3-TS transmission protocols. The obtained asymptotic expressions are useful in analyzing the average error probability at high SNR in the next section.

Corollary 1: The asymptotic outage probability at the secondary source in the 2-TS and 3-TS protocols for a two-way AF relaying based distributed ZFB in spectrum-sharing system is given by

$$\begin{aligned} P_{out\infty}^{\tau-TS} &\approx \left(\frac{(L_s - M + 1)\gamma_{th}^{L_s-M+1}}{\lambda_{s_i,p}^{L_s-M+1}} + \frac{c\gamma_{th}^{L_s-M}}{\Gamma(L_s - M + 1)} \right) \\ &\times \left(\frac{1}{\gamma_{q_i}} \right)^{L_s-M} + o(\gamma_{th}^2), \end{aligned} \quad (40)$$

where $\tau = 2, 3$, $i = 1, 2$, respectively, $c = (\alpha\gamma_r)^{L_s-M+2}$ where $\alpha = 1$ for 2-TS and $o(\gamma_{th}^2)$ stands for higher-order terms.

Proof: The technique developed in [41] can be used to find asymptotic behavior of $P_{out}^{\tau-TS}$ at high SNR. First, we find the approximate CDFs of the total received SNR at S_j , $\gamma_{eq}^{\tau-TS}$. Recalling (20) and (24), we make use of the infinite series representation of the incomplete Gamma function as in [34, Eq. 8.354.2]

$$\Gamma(\theta, x) = \Gamma(\theta) - \sum_{n=0}^{\infty} \frac{(-1)^n x^{\theta+n}}{n!(\theta+n)}. \quad (41)$$

which leads to

$$\Gamma(\theta, x) \stackrel{x \rightarrow 0}{\approx} \Gamma(\theta) - \frac{x}{\theta}. \quad (42)$$

Therefore, using the mutual independence between h_{s_1, r_i} , f_{s_2, r_i} ($i = 1, \dots, L_s$), $h_{s_1, p}$, $h_{s_2, p}$ and g_{r_i, p_m} , ($m = 1, \dots, M$) and by using Taylor's series, the approximate CDF of $\gamma_{eq}^{\tau-TS}$, denoted by $F_{\gamma_{eq}^{\tau-TS}}(\gamma)$, can be written as

$$F_{\gamma_{eq}^{\tau-TS}}(\gamma) \approx \left(\frac{\gamma^{L_s-M+1}}{\lambda_{s_i, p}^{L_s-M+1}} + \frac{c\gamma^{L_s-M}}{\Gamma(L_s-M+1)} \right) \left(\frac{1}{\gamma_{q_i}} \right)^{L_s-M}. \quad (43)$$

Finally, by computing $F_{\gamma_{eq}^{\tau-TS}}(\gamma)|_{\gamma=\gamma_{th}}$, we get (40), thus completes the proof.

It can be observed from (40) that the diversity order is $L_s - M$. This means that the diversity gain increases linearly with the number of the secondary relays. Furthermore, as the number of the primary receivers increases, the outage probability increases. Meanwhile, as the value of Q increases, the outage probability decreases. We remark that M spatial degrees of freedom of the L_s single antenna relays are used for interference suppression as a condition to perform ZFB, which leads to $(L_s - M)$ diversity gain.

VII. AVERAGE ERROR PROBABILITY ANALYSIS

In this section, we derive expressions for the end-to-end of average error probability performance for both 2-TS and 3-TS.

A. 2-TS Protocol

Theorem 3: A closed-form expression for the average error probability in the 2-TS protocol for a two-way AF relaying based distributed ZFB in spectrum-sharing system is given by

$$P_e^{2-TS} = \frac{1}{2} - \frac{1}{2\sqrt{\pi}} \bar{\delta} \sum_{m=0}^{M-L_s-2} \frac{1}{c^m m!} \left(\frac{1}{A} \right)^{v+\frac{3}{4}} \times G_{4,4}^{4,1} \left(\frac{b^2}{A} \middle|_{L_s-M, 0, 0, -L_s+M}^{-v-\frac{1}{4}, 0, \frac{1}{2}, -v+\frac{1}{4}} \right), \quad (44)$$

where $\bar{\delta} = \delta(M - L_s - 2)!$, $\delta = 4(L_s - M + 1)\gamma_r^{-(L_s-M)}/c^{L_s-M+1}(\Gamma(L_s-M))^2$, $v = 2L_s - 2M + m + (3/4)$, $A = 1$ (for binary phase shift keying (BPSK) modulation), $c = \lambda_{s_1, p}\gamma_{q_1}$ and $b = 2/\sqrt{\gamma_r}$.

Proof: To obtain the average error probability for the secondary system, the MGF based approach will be used in this paper. Let $(\gamma_{eq}^{2-TS})^{-1} = \gamma_{1,2TS}^{-1} + (\gamma_{2,2TS}/\gamma_{1,2TS}\gamma_{3,2TS}) + \gamma_{3,2TS}^{-1} = X_1 + X_2 + X_3$ where $X_1 = \gamma_{1,2TS}^{-1}$, $X_2 = \gamma_{2,2TS}/\gamma_{1,2TS}\gamma_{3,2TS}$ and $X_3 = \gamma_{3,2TS}^{-1}$. As $(\gamma_{eq}^{2-TS})^{-1}$ is the sum of three independent random variables, the MGF of the $(\gamma_{eq}^{2-TS})^{-1}$, denoted by $\phi_{(\gamma_{eq}^{2-TS})^{-1}}(s)$, results simply from the product of the three MGFs of X_1 , X_2 , and X_3 , denoted as $\phi_{X_1}(s)$, $\phi_{X_2}(s)$ and $\phi_{X_3}(s)$, respectively. The MGF of random variable X with PDF $f_X(x)$ is defined as

$$\phi_X(s) = \int_0^{\infty} e^{-sx} f_X(x) dx, \quad (45)$$

We first need to find the PDFs of X_1 , X_2 and X_3 . For the PDF of X_1 , we derive it in the same way we did in (25), which after a few mathematical manipulations, is obtained as [13]

$$f_{X_1}(x) = \frac{\lambda_{s_1, p}(L_s - M + 1)}{(\gamma_{q_1})^{L_s-M+1} \left(\lambda_{s_1, p} x + \frac{1}{\gamma_{q_1}} \right)^{L_s-M+2}}. \quad (46)$$

Without loss of generality, we assume here that both of the sources have the same maximum transmission powers, i.e., $P_{s_1} = P_{s_2}$. Considering that $X_2 = 1/\gamma_r \|\Xi^\perp \mathbf{h}\|^2$, which is an inverse chi-square random variable with $2(L_s - M)$ degrees of freedom, the PDF of X_2 is given as

$$f_{X_2}(x) = \frac{e^{-\frac{1}{\gamma_r x}}}{(\gamma_r)^{L_s-M} (L_s - M - 1)! x^{L_s-M+1}}. \quad (47)$$

Similarly, the PDF of X_3 is the PDF of the inverse chi-square random variable, which also leads to the following expression

$$f_{X_3}(x) = \frac{e^{-\frac{1}{\gamma_r x}}}{(\gamma_r)^{L_s-M} (L_s - M - 1)! x^{L_s-M+1}}. \quad (48)$$

Substituting (46) into (45), and using [34, 3.382.4], the MGF for X_1 is

$$\phi_{X_1}(s) = \frac{L_s - M + 1}{c^{L_s-M+1}} s^{L_s-M+1} e^{\frac{s}{c}} \Gamma \left(-L_s + M - 1, \frac{s}{c} \right). \quad (49)$$

Similarly, substituting (47) and (48) into (45), and using [34, 3.471.9], the MGFs for X_2 and X_3 are

$$\phi_{X_j}(s) = \frac{2(\gamma_r)^{-(L_s-M)}}{\Gamma(L_s-M)} (\gamma_r s)^{\frac{L_s-M}{2}} K_{L_s-M} \left(2\sqrt{\frac{s}{\gamma_r}} \right), \quad (50)$$

where $K_v(\cdot)$ is the modified Bessel function [34]. Now, we can easily find the MGF of $(\gamma_{eq}^{2-TS})^{-1}$ as the product of $\phi_{X_1}(s)$, $\phi_{X_2}(s)$ and $\phi_{X_3}(s)$, which is given as

$$\phi_{(\gamma_{eq}^{2-TS})^{-1}}(s) = \delta s^{2L_s-2M+1} e^{\frac{s}{c}} \Gamma \left(-L_s + M - 1, \frac{s}{c} \right) \times \left(K_{L_s-M} \left(2\sqrt{\frac{s}{\gamma_r}} \right) \right)^2. \quad (51)$$

By representing the incomplete Gama function into another mathematical form using [34, 3.352.2], (51) simplifies to

$$\phi_{(\gamma_{eq}^{2-TS})^{-1}}(s) = \delta(M - L_s - 2)! \sum_{m=0}^{M-L_s-2} \frac{s^{2L_s-2M+1+m}}{c^m m!} \times \left(K_{L_s-M} \left(2\sqrt{\frac{s}{\gamma_r}} \right) \right)^2. \quad (52)$$

We utilize the following formula to compute the MGF of the γ_{eq}^{2-TS} exploiting the MGF of $(\gamma_{eq}^{2-TS})^{-1}$ [35, Eq. 18]

$$\phi_{\gamma_{eq}^{2-TS}}(s) = 1 - 2\sqrt{s} \int_0^\infty J_1(2\beta\sqrt{s}) \phi_{(\gamma_{eq}^{2-TS})^{-1}}(\beta^2) d\beta, \quad (53)$$

where $J_1(\cdot)$ is the Bessel function of the first kind [34]. Despite seeming difficult, this formula can still be used to study the performance of the average error probability based on the relationship that exists between the MGF and the symbol error rate [33]. Utilizing the MGF-based form, the average error probability of coherent binary signaling is given by [33, Eq. 9.15]

$$P_e^{2-TS} = \frac{1}{\pi} \int_0^{\pi/2} \phi_{\gamma_{eq}^{2-TS}} \left(\frac{A}{\sin^2 \varphi} \right) d\varphi, \quad (54)$$

where $A = 1$ for BPSK. Substituting (53) into (54) and after some manipulations, the formula of the error probability becomes

$$P_e^{2-TS} = \frac{1}{2} - \frac{2}{\pi} \int_0^\infty \phi_{(\gamma_{eq}^{2-TS})^{-1}}(\beta^2) \int_0^{\pi/2} \sqrt{\frac{A}{\sin^2 \varphi}} \times J_1 \left(\sqrt{\frac{4\beta^2 A}{\sin^2 \varphi}} \right) d\varphi d\beta. \quad (55)$$

The inner integral of (55) can be solved by using the variable change and equation [36, eq. 2.12.4.15] which results in the value $(\sin(2\beta\sqrt{A})/2\beta)$. So the error probability can be evaluated according to the following formula

$$P_e^{2-TS} = \frac{1}{2} - \frac{2}{\pi} \underbrace{\int_0^\infty \phi_{(\gamma_{eq}^{2-TS})^{-1}}(\beta^2) \frac{\sin(2\beta\sqrt{A})}{2\beta} d\beta}_{I_4}, \quad (56)$$

where $\phi_{(\gamma_{eq}^{2-TS})^{-1}}$ is the MGF of the inverse SNR given in (52).

We put I_4 in the following format

$$I_4(\nu, \mu, a_1, \lambda_1, \lambda_2, b_1, b_2) = \int_0^\infty s^\nu J_\mu(a\sqrt{s}) \times K_{\lambda_1}(b_1\sqrt{s}) K_{\lambda_2}(b_2\sqrt{s}) ds. \quad (57)$$

To continue, we make use of the identity

$$\sin(2\beta\sqrt{A}) = \sqrt{\pi\beta\sqrt{A}} J_{\frac{1}{2}} \left(\sqrt{4\beta^2\sqrt{A}} \right). \quad (58)$$

By incorporating (52) and (58) into (56), the format of I_4 in (56) becomes as in (58), that is,

$$I_4 = \int_0^\infty \delta(M - L_s - 2)! \sum_{m=0}^{M-L_s-2} \frac{\beta^{2(2L_s-2M+m+\frac{3}{4})}}{c^m m!} \times \frac{\sqrt{\pi\sqrt{A}}}{2} J_{\frac{1}{2}} \left(\sqrt{4\beta^2\sqrt{A}} \right) \left(K_{L_s-M} \left(2\sqrt{\frac{\beta^2}{\gamma_r}} \right) \right)^2 d\beta. \quad (59)$$

By solving I_4 in (60) using [37], a closed-form expression for the BER in the 2-TS protocol is shown as in (44). This completes the proof. \square

B. 3-TS Protocol

Following the same steps used in the 2-TS protocol, the MGF based approach is used to obtain the average error probability expression in the 3-TS protocol. Let $(\gamma_{eq}^{3-TS})^{-1} = \gamma_{1,3TS}^{-1} + (\gamma_{2,3TS}/\gamma_{1,3TS}\gamma_{3,3TS}) + \gamma_{3,3TS}^{-1} = Y_1 + Y_2 + Y_3$ where $Y_1 = \gamma_{1,2TS}^{-1}$, $Y_2 = \gamma_{2,2TS}/\gamma_{1,2TS}\gamma_{3,2TS}$ and $Y_3 = \gamma_{3,2TS}^{-1}$. As $(\gamma_{eq}^{3-TS})^{-1}$ is the sum of three independent random variables, the MGF of the $(\gamma_{eq}^{3-TS})^{-1}$, denoted by $\phi_{(\gamma_{eq}^{3-TS})^{-1}}(s)$, is $\phi_{(\gamma_{eq}^{3-TS})^{-1}}(s) = Y_1 \times Y_2 \times Y_3$. For the PDF of Y_1 , we derive it in the same way as applied in (46), which after a few mathematical manipulations, is obtained as [13]

$$f_{Y_1}(x) = \frac{\lambda_{s_1,p} L_s}{(\gamma_{q_1})^{L_s} \left(\lambda_{s_1,p} x + \frac{1}{\gamma_{q_1}} \right)^{L_s+1}}. \quad (60)$$

Considering the same maximum power constraints, $Y_2 = \|\mathbf{f}\|^2/\gamma_{r_1} \|\mathbf{\Xi}^\perp \mathbf{f}\|^2 \|\mathbf{h}\|^2$, which is a ratio between a chi-square random variable and a product of two chi-square random variables. The PDF of Y_2 is obtained using [38, eq. 22] which after few mathematical manipulations results in

$$f_{Y_2}(x) = \left(\frac{1}{\gamma_{r_1}} \right)^{\frac{(2L_s-M-1)}{2}} \frac{x^{-\frac{(2L_s-M+1)}{2}}}{(\Gamma(L_s))^2 \Gamma(L_s - M)} \times G_{2,1}^{1,2} \left(\gamma_{r_1} x \left| \begin{matrix} \frac{(1+M)}{2}, \frac{(1-M)}{2} \\ \frac{(4L_s-M-1)}{2} \end{matrix} \right. \right). \quad (61)$$

The PDF of Y_3 is the same as the one in (48). Substituting (60) into (45), and using [34, 3.382.4], the MGF for Y_1 is

$$\phi_{Y_1}(s) = \frac{L_s}{c L_s} s^{L_s} e^{\frac{s}{c}} \Gamma \left(L_s, \frac{s}{c} \right). \quad (62)$$

Similarly, substituting (61) into (45) and representing the exponential part in terms of Meiger's G-function using [39, eq. 11] as $e^{-sx} = G_{0,1}^{1,0}(sx|_0^-)$, $\phi_{Y_2}(s)$ is expressed as

$$\phi_{Y_2}(s) = \int_0^\infty (\gamma_{r_1})^{-\frac{(2L_s-M-1)}{2}} \frac{x^{-\frac{(2L_s-M+1)}{2}}}{(\Gamma(L_s))^2 \Gamma(L_s - M)} \times G_{2,1}^{1,2} \left(\gamma_{r_1} x \left| \begin{matrix} \frac{(1+M)}{2}, \frac{(1-M)}{2} \\ \frac{(4L_s-M-1)}{2} \end{matrix} \right. \right) G_{0,1}^{1,0} \left(sx \left| \begin{matrix} - \\ 0 \end{matrix} \right. \right) dx. \quad (63)$$

Knowing that the integral of the product of two Meijer's G-functions and a power term results also in a Meijer's G-function [39, eq. 21], $\phi_{Y_2}(s)$ simplifies to

$$\phi_{Y_2}(s) = \frac{1}{(\Gamma(L_s))^2 \Gamma(L_s - M)} G_{1,3}^{3,1} \left(\frac{s}{\gamma_{r_1}} \middle|_{0, L_s - M, L_s}^{1 - L_s} \right). \quad (64)$$

The MGF for Y_3 is the same as the one in (50). We can now easily find the MGF $\phi_{(\gamma_{eq}^{3-TS})^{-1}}$ as

$$\begin{aligned} \phi_{(\gamma_{eq}^{3-TS})^{-1}}(s) &= \delta_1 s^{\frac{3L_s - M}{2}} e^{\frac{s}{c}} \Gamma \left(L_s, \frac{s}{c} \right) K_{L_s - M} \left(2\sqrt{\frac{s}{\gamma_{r_1}}} \right) \\ &\quad \times G_{1,3}^{3,1} \left(\frac{s}{\gamma_{r_1}} \middle|_{0, L_s - M, L_s}^{1 - L_s} \right), \end{aligned} \quad (65)$$

where $\delta_1 = (2L_s(\gamma_{r_1})^{-(L_s - M/2)}/c^{L_s}(\Gamma(L_s))^2)$. Again, utilizing the relationship that exists between the MGF and symbol error rate [33], the average error probability in the 3-TS protocol can be evaluated according to the following formula

$$P_e^{3-TS} = \frac{1}{2} - \frac{2}{\pi} \int_0^{\infty} \phi_{(\gamma_{eq}^{3TS})^{-1}}(\beta^2) \frac{\sin(2\beta\sqrt{A})}{2\beta} d\beta, \quad (66)$$

where $\phi_{(\gamma_{eq}^{3-TS})^{-1}}$ is the MGF of the inverse SNR given in (65). Unfortunately, the integral in (66) is difficult to evaluate. Therefore, we tackle it using the Gauss-Laguerre quadrature numerical integration as follows [40]:

$$P_e^{3-TS} \approx \frac{1}{2} - \frac{2}{\pi} \sum_{j=1}^J w_j f(A, x_j), \quad (67)$$

where J is the number of interpolation points, x_j are the j th zeros of the Laguerre polynomial $L_n(x)$, w_j are the associated weights given by

$$w_j = \frac{(n!)^2 x_j}{(n+1)^2 L_{n+1}(x_j)^2} \quad (68)$$

and

$$f(A, x_j) = e^x \phi_{(\gamma_{eq}^{3TS})^{-1}}(x^2) \frac{\sin(2x\sqrt{A})}{2x}. \quad (69)$$

The approximate BER expression in (67) gives high accuracy results, which will be clear in the subsequent numerical results section.

Remark: Using $\phi_{(\gamma_{eq}^{2-TS})^{-1}}(s)$ and $\phi_{(\gamma_{eq}^{3-TS})^{-1}}(s)$ derived in (51) and (65) respectively, and with the help of the formula in (53), the average error probability can be evaluated for different modulation schemes such as M-ary phase shift keying (M-PSK) and M-ary quadrature amplitude modulation (M-QAM) [33]. For example, the average symbol error rate (SER) for M-PSK can be obtained as [34, Eq. 9.15]

$$P_e^{\tau-TS} = \frac{1}{\pi} \int_0^{(M-1)\pi/M} \phi_{\gamma_{eq}^{\tau-TS}} \left(\frac{A}{\sin^2 \varphi} \right) d\varphi, \quad (70)$$

where $A = \sin^2(\pi/M)$ and $\tau = 2, 3$. Furthermore, (55) can be upper bounded by a simple form as in [34, Eq. 9.27]

$$P_e^{\tau-TS} \leq (1 - 1/M) \phi_{\gamma_{eq}^{\tau-TS}}(A) \quad (71)$$

The equivalent average bit error probability for M-ary PSK assuming Gray coding is well approximated as [34, (5.2.62)]

$$P_b^{\tau-TS} \approx \frac{P_e^{\tau-TS}}{\log_2 M}. \quad (72)$$

C. Asymptotic Average Bit Error Probability

To gain key insights, we consider the average bit error probability at high SNR.

Corollary 2: The asymptotic average bit error probability at the secondary source S_j in the 2-TS and 3-TS protocols for a two-way AF relaying based distributed ZFB in spectrum-sharing system is obtained by

$$\begin{aligned} P_e^{\tau-TS} &\approx \frac{a\sqrt{b}}{2\sqrt{\pi}} \left(\frac{\Gamma(L_s - M + \frac{3}{2})}{c\lambda_{s_i,p}^{L_s - M + 1} b^{L_s - M + \frac{3}{2}}} \right. \\ &\quad \left. + \frac{c\Gamma(L_s - M + \frac{1}{2})}{\Gamma(L_s - M + 1)b^{L_s - M + \frac{1}{2}}} \right) \left(\frac{1}{\gamma_{q_i}} \right)^{L_s - M}, \end{aligned} \quad (73)$$

where $\tau = 2, 3$, $i = 1, 2$, $c = (\alpha\gamma_r)^{L_s - M + 2}$ where $\alpha = 1$ for 2-TS and (a, b) values depend on the modulation scheme.

Proof: The asymptotic error probability can be given through

$$P_{e\infty}^{\tau-TS} \approx \frac{a\sqrt{b}}{2\sqrt{\pi}} \int_0^{\infty} \frac{e^{-bu}}{\sqrt{u}} F_{\gamma_{eq\infty}}^{\tau-TS}(u) du. \quad (74)$$

where $F_{\gamma_{eq\infty}}^{\tau-TS}(u)$ is the approximate CDF as $\gamma_{q_i} \rightarrow \infty$. Utilizing (43) combined with *Corollary 1* and after doing the integration, we get (73). This concludes the proof. \square

Similar to the asymptotic outage probability case, (73) suggests the same diversity gain $L_s - M$ with similar conclusions. We remark that this diversity gain is achieved in the regime where there is a constraint on Q , not on P_{s_j} . However, if P_{s_j} is limited, an error floor will occur and hence the diversity gain approaches zero at high SNRs.

D. Power Allocation at the Relays

In this section, the design of the power allocation parameter α at the secondary relays is investigated. The objective is to pick α such that the minimum average error probability at the two secondary transceivers is achieved. Specifically, α is chosen according to the optimization problem:

$$\begin{aligned} \alpha_{opt} &= \arg \min_{\alpha} (P_e^{3-TS, S_2}(\alpha) + P_e^{3-TS, S_1}(\alpha)) \\ &\text{subject to } 0 < \alpha < 1 \end{aligned} \quad (75)$$

where P_e^{3-TS, S_2} and P_e^{3-TS, S_1} are the average error probability at S_2 and S_1 , respectively and can be obtained from (56). Obtaining a closed-form expression for the solution to (75) is not easy. As an alternative, it can be solved numerically as we will show later. Obviously the sum average error probability is minimized when α_{opt} is used, and this yields better performance compared to the case when α is fixed.

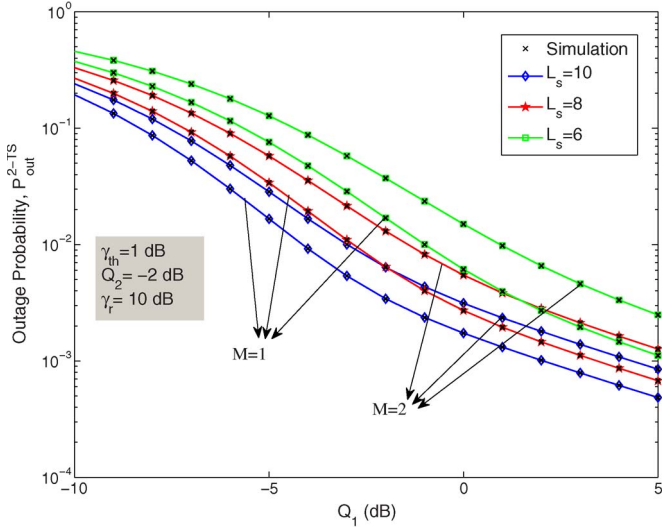


Fig. 2. Outage probability vs. Q_1 (dB) for the 2-TS protocol for $L_s = 6, 8, 10$ and $M = 1, 2$.

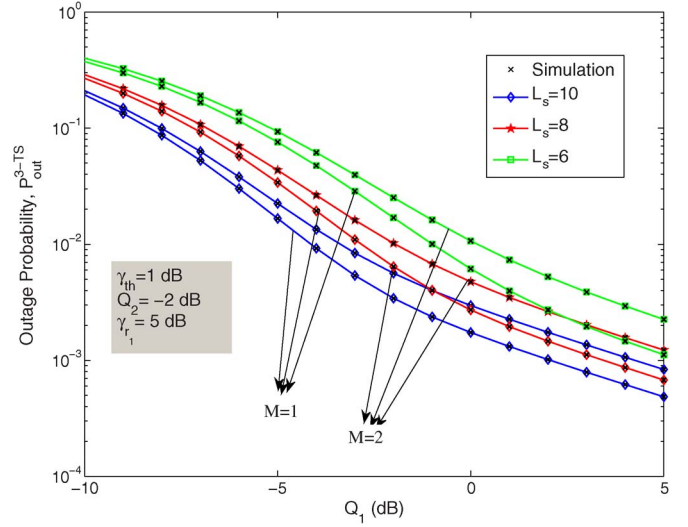


Fig. 3. Outage Probability vs. Q_1 (dB) for the 3-TS protocol for $L_s = 6, 8, 10$ and $M = 2, 3$.

VIII. NUMERICAL RESULTS AND DISCUSSION

In this section, we investigate the performance of the derived results through numerical examples and simulations. Unless otherwise stated, the distance between the sources equals d . Let d_{S_j, R_i} denote the distance from S_j to the i th relay, and hence, $d_{S_1, R_i} = d - d_{S_2, R_i}$. We assume that the relays are located on a straight line vertical to the distance between the two sources, however, the results and conclusions of this paper extend to any setting. Furthermore, the path loss exponents is set to four. The channel mean power for the links from PUs to the secondary nodes is defined by the locations, as $\lambda_{r_i, p} = (\sqrt{d_x^2 + d_y^2})^{-4}$, where (d_x, d_y) are the coordinates of the PUs. We also assume that $\lambda_{s_1, p} = \lambda_{s_2, p} = 1$. It is also assumed that the range of the power transmission of S_1 and S_2 is limited according to the peak power constraints that were mentioned in the system model.

A. Effects of ZFB, Number of Relays and Number of PUs on the Performance

Figs. 2 and 3 show the outage performance of S_2 versus Q_1 for $L_s = 6, 8, 10$, $M = 1, 2$ at $\gamma_{th} = 1$ dB, $\gamma_{q_2} = -2$ dB, $\gamma_r = 10$ dB and $\gamma_{r_1} = 5$ dB. As observed from the figures, as the value of Q_1 increases, the outage performance improves substantially. Moreover, by increasing the number of relays with ZFB, we observe significant improvements in the outage performance. This is attributed to the combined cooperative diversity and beamforming which enhances the total received SNR at the transceiver. Clearly, as the number of existing PUs increases from one to two, the outage performance becomes worse because the secondary sources have to adapt their transmit powers according to the most affected PU.

In Fig. 4, we simulate the outage system performance using the exact received SNR and the approximate received SNR in (9), assuming the negligible noise term. It is observed from the figure that there is a small gap between both curves at low Q values due to neglecting the noise term. As Q increases, the

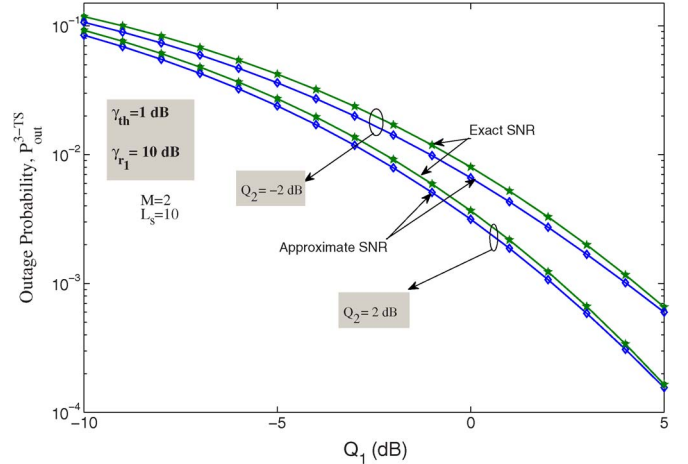


Fig. 4. Outage probability of 3-TS protocol using the exact and approximate received SNR.

curves almost overlap. To conclude, neglecting the noise term does not affect the system performance.

Figs. 5 and 6 illustrate the average bit error probability performance versus $Q_1 = Q_2 = Q$ for $L_s = 6, 8, 10$ and $M = 1, 2, 3$, $\gamma_r = \gamma_{r_1} = 5$ dB at $\gamma_{th} = 1$ dB. It is obvious that the average bit error probability performance improves substantially as the number of relays increases and Q becomes looser. With beamforming and increasing the number of relays, the gain becomes more. The larger the number of existing PUs, the worse the error probability, as expected.

In Fig. 7, we simulate the average bit error probability for both approximate and exact received SNRs. It is clear that there is a small gap between the two curves, which confirms the validity of the assumption used in the paper.

B. Comparison Between 2-TS and 3-TS

For a fair comparison, we fix the total transmit power at the relays, i.e., P_r and the total available power at both transceivers, $P_{s_1} + P_{s_2}$. Hence, for the 4-TS protocol, we use $P_r/2$ in the second and fourth time slots to keep the total power the same.

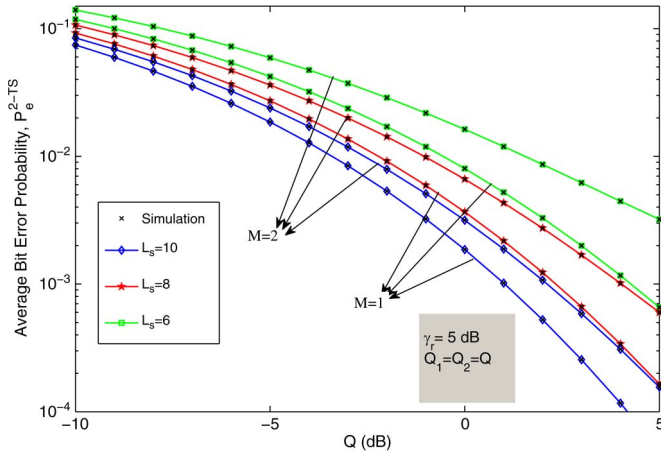


Fig. 5. Average bit error probability vs. Q (dB) for the 2-TS protocol for $L_s = 6, 8, 10$ and $M = 1, 2$.

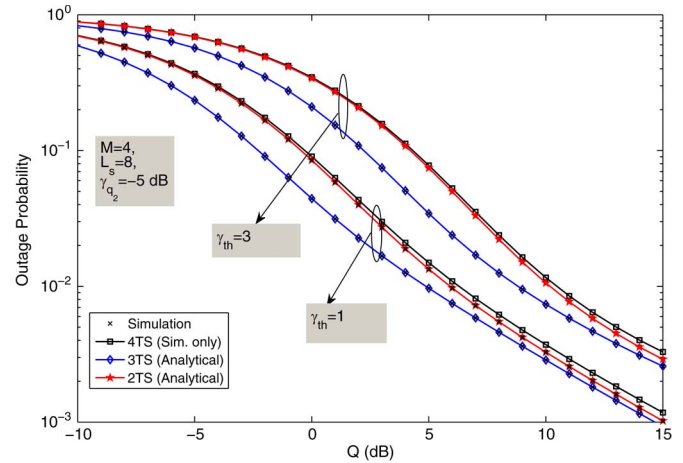


Fig. 8. Outage probability vs. Q (dB) for the 2-TS, 3-TS and 4-TS protocols, with $L_s = 8$ and $M = 4$.

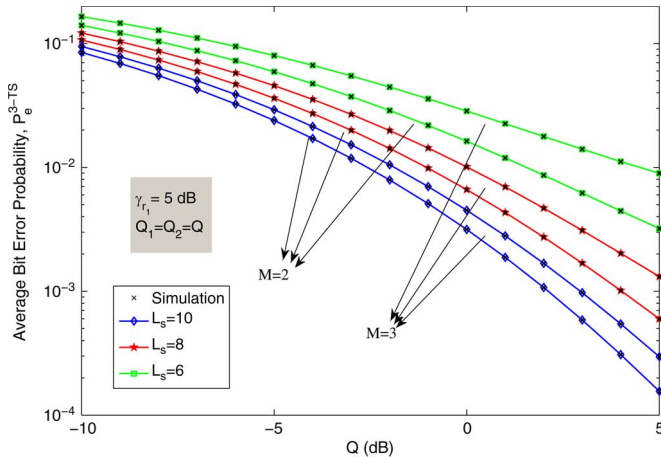


Fig. 6. Average bit error probability vs. Q (dB) for the 3-TS protocol for $L_s = 6, 8, 10$ and $M = 2, 3$.

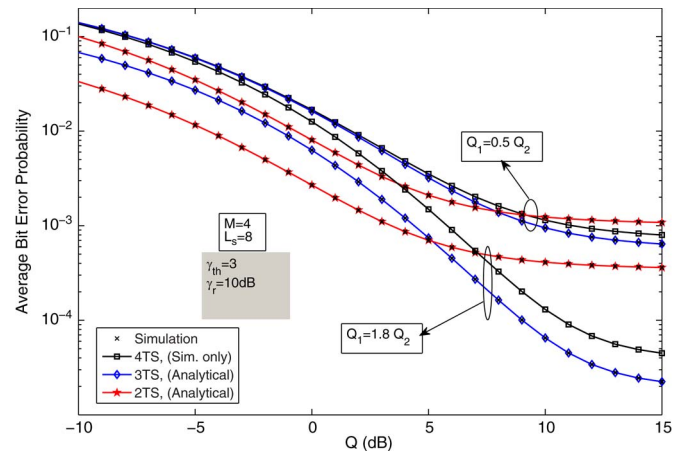


Fig. 9. Average bit error probability vs. Q (dB) for the 2-TS with (QPSK) 3-TS with (8-PSK) and 4-TS with (16-PSK) protocols, $L_s = 8$ and $M = 4$.

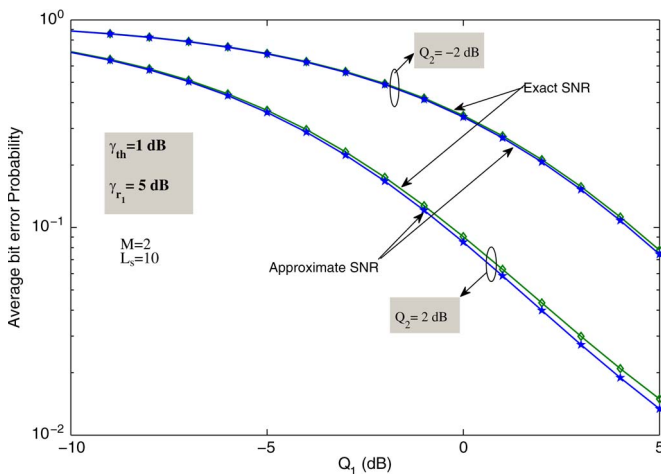


Fig. 7. Average bit error probability of 3-TS protocol using the exact and approximate received SNR.

In Fig. 8, the outage probability for the 2-TS, 3-TS and 4-TS protocols is investigated. We use $\gamma_{r1} = 0.5\gamma_r$, $L_s = 7, 8$, $M = 4$ at two different SNR thresholds $\gamma_{th} = 1, 3$ dB. It can be readily seen that the outage performance in the 3-TS protocol performs better than that of the 2-TS and 4-TS protocols for

the same values of L_s , M and γ_{th} . This offers a good trade-off between the system performance and bandwidth efficiency. It is also clear from the figure that as γ_{th} goes from one to three, the curves shift up implying worse performance.

For a fair comparison in the average bit error probability curves, we use two different modulation schemes to maintain the same spectral efficiency. We use quadrature phase shift keying (QPSK), 8-PSK and 16-PSK modulation schemes for the 2-TS, 3-TS and 4-TS transmission protocols, respectively. Fig. 9 shows a plot for the average bit error probability versus Q_2 of both 2-TS, 3-TS and 4-TS for varying values of Q_1 , $L_s = 6, 8$ and $M = 4$. The analytical results are based on (72). For the 3-TS protocol, we use the optimum values of α according to (75) obtained only by simulations which minimize the average error probability at both transceivers. We notice that when the values of Q_2 increases from 0 to 10, the 3-TS protocol performs better than the 2-TS protocol when $Q_1 = 1.8Q_2$ and also when $Q_1 = 0.5Q_2$. This is due to the reason that, in 3-TS, the different transmit powers at transceivers S_1 and S_2 lead to a different power weighting at the relays. The transceiver with a higher transmit power will be weighted more at the relay than the transceiver with a lower transmit power. This is not the case in the 2-TS and 4-TS where the received

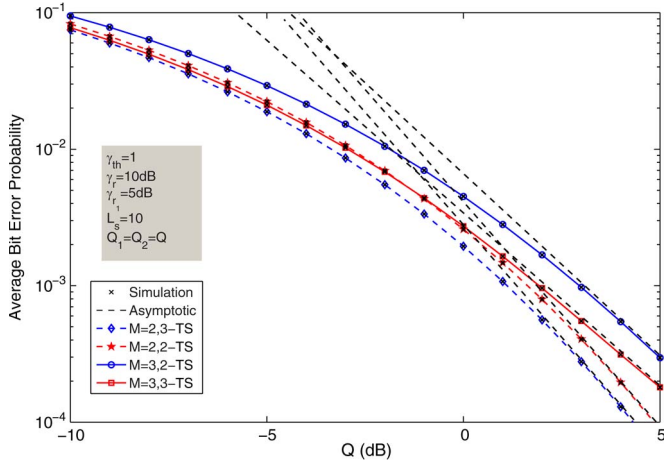


Fig. 10. Asymptotic average bit error probability vs. Q_2 (dB) for the 2-TS and 3-TS protocols, $L_s = 10$ and $M = 2, 3$ using BPSK.

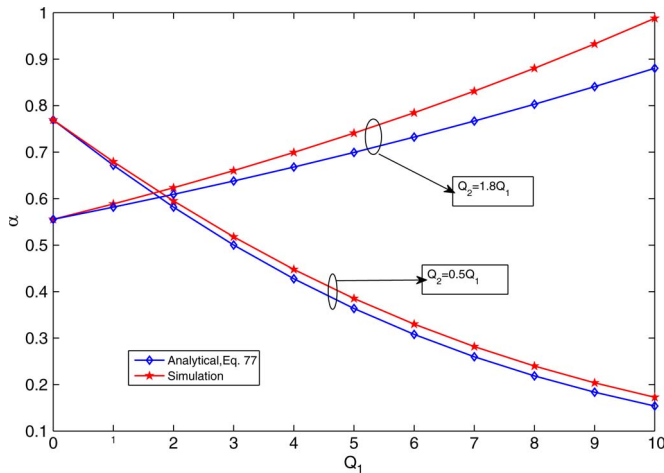


Fig. 11. Power allocation parameter α vs. Q_2 (dB) for the 3-TS protocol, $L_s = 6$ and $M = 3$, and $P_r = 10$ dB.

signals from both transceivers are weighted equally and thus can not make use of the different transmit power to improve the system performance [7]. This highlights a good advantage that the 3-TS is effective when the transmit powers at the transceivers are different. This is a practical scenario since in underly cognitive radio networks, the transceivers' powers vary, depending on the interference constraints.

Fig. 10 shows the asymptotic average bit error probability performance of the 2-TS and 3-TS protocol versus Q assuming $\gamma_r = 10$, $L_s = 10$, $M = 2, 3$ at $\gamma_{th} = 1$ dBs. We see a good match between the asymptotic results based on (73) and the simulation results. Observations and conclusions similar to the ones made for the other figures hold for this figure. Based on the analytical results in (73), it is clear that the diversity gain of both schemes for the given parameters is the same.

In Fig. 11, we plot the optimal values of α for the 3-TS protocol as function of Q_2 for different values of Q_1 . As explained in the analytical section, the value of α increases or decreases with Q_1 . The signal broadcasted by the transceiver with a higher transmit power will be weighted more at the relays than the signal broadcasted by the transceiver with lower transmit power. Meanwhile, in the 2-TS protocol, the received

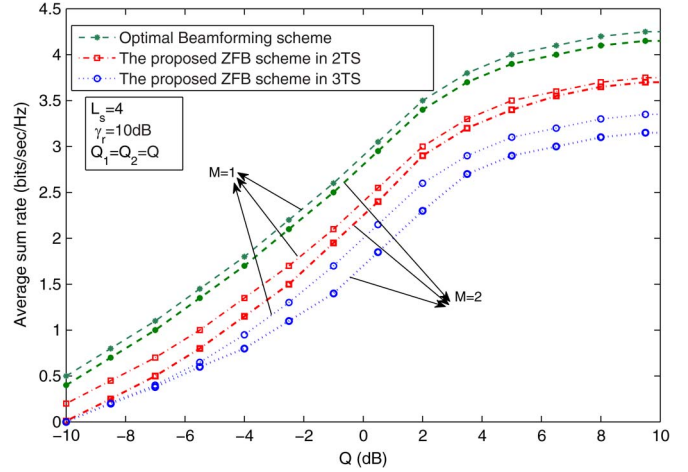


Fig. 12. Average sum rate comparison between the proposed ZFB scheme and the optimal beamforming scheme, with $L_s = 4$ and $M = 1, 2$.

signals at the relays are weighted equally. Note that the curves are not matching at high values of Q_2 because one curve results from simulations whereas the other is obtained analytically at high values of Q_2 . However, they have the same trend.

C. Comparison Between the Sub-optimal ZFB Beamforming Scheme and the Optimal Beamforming Scheme

In Fig. 12, the performance of the achievable sum-rate for the 2-TS and 3-TS protocols employing the ZFB scheme is compared (the achievable sum-rate curve is generated by simulations, where over 50,000 channel realizations were generated and averaged) with the one that employed optimal beamforming scheme, e.g., [22]. The optimization problem for the system in [22] is to maximize the sum-rate of both transceivers subject to power constraints. The system is a two-way multi-antenna relay channel that transmits over two time-slots. For comparison, we assume that the total power available at the relay(s) is the same, the number of antennas in [22] is equal to the number of relays $L_s = 4$ in our system and $M = 1, 2$. It is observed that there is a 1-dB gap between the performance of the adopted ZFB scheme and the optimal beamforming scheme. However, our proposed scheme offers a good performance at lower complexity in addition to being practically implementable if compared to the optimal scheme. The figure also clarifies that 2-TS is better than the 3-TS protocol in terms of bandwidth efficiency, which is expected. Although adding one more time-slot in the 3-TS protocol enhances the performance in terms of the outage and error probabilities, the bandwidth efficiency of 2-TS protocol is still better.

To compare the complexity between the proposed scheme and the optimal scheme, we note that the ZFB vector has a small fixed complexity, requiring only one matrix inversion Ξ^\perp and one matrix multiplication to obtain the beamforming weights. However, in the optimal scheme in [22], an iterative numerical optimization technique is used which converges within 20–30 iterations. Within each of these iterations, a number of matrix multiplications, matrix inversions, and vector 2-norm calculations for each user are needed to find the solution. So the computational complexity of the two schemes is not comparable.

IX. CONCLUSION

We investigated a cooperative two-way AF relaying system model in a spectrum sharing environment. The proposed system limits the interference to the primary users using a distributed ZFB approach and peak interference power constraints. The beamforming weights were optimized to maximize the received SNR at both secondary transceivers and to null the interference inflicted on the primary users. We considered two transmission protocols over two time-slots and three time-slots. It is often expected that the three time-slot protocol is subordinate to the two time-slot protocol due to the loss in the data rate. Such a comparison, however, ignores the fact the 3-TS protocol benefits from one additional degree of freedom per relay. To clarify the potential advantages of 3-TS and 2-TS transmission protocols and study the performance tradeoffs of both of them in spectrum sharing systems, we investigated the performance of the secondary system by deriving closed-form expressions for the outage and average error probabilities. We compared the performance of the two protocols in terms of the outage probability, average error probability and average sum-rate. When compared to the performance of the optimal beamforming scheme, the adopted sub-optimal ZFB scheme performance is somehow close to that of the optimal one in terms of the average sum-rate performance. Our numerical results showed that the distributed ZFB method enhances the outage and error probabilities by increasing the number of participating relays in addition to limiting interference to the PUs. In addition, our results showed that the 3-TS protocol outperforms the 2-TS protocol in certain scenarios, which was clear in the outage and error probabilities performance. As a result, the 3-TS protocol offers a good compromise between bandwidth efficiency and system performance. As an extension, an adaptive 2-TS/3-TS system could be adopted to enhance both the bandwidth efficiency and reliability.

REFERENCES

- [1] A. Goldsmith, S. A. Jafar, I. Maric, and S. Srinivasa, "Breaking spectrum gridlock with cognitive radios: An information theoretic perspective," *Proc. IEEE*, vol. 97, no. 5, pp. 894–914, May 2009.
- [2] S. Haykin, "Cognitive radio: Brain-empowered wireless communications," *IEEE J. Sel. Areas Commun.*, vol. 23, no. 9, pp. 201–220, Feb. 2005.
- [3] T. M. Duman and A. Ghrayeb, *Coding for MIMO Communication Systems*. Hoboken, NJ, USA: Wiley, Jan. 2008.
- [4] X. Zeng, A. Ghrayeb, and M. Hasna, "Joint optimal threshold-based relaying and ML detection in network-coded two-way relay," *IEEE Trans. Commun.*, vol. 60, no. 9, pp. 2657–2667, Sep. 2012.
- [5] G. Al-Habian, A. Ghrayeb, M. Hasna, and A. Abu-Dayya, "Threshold-based relaying in coded cooperative networks," *IEEE Trans. Veh. Technol.*, vol. 60, no. 1, pp. 123–135, Jan. 2011.
- [6] S. Nguyen, A. Ghrayeb, G. Al-Habian, and M. Hasna, "Mitigating error propagation in two-way relay channels employing network coding," *IEEE Trans. Wireless Commun.*, vol. 9, no. 11, pp. 3380–3390, Nov. 2010.
- [7] R. H. Y. Louie, Y. Li, and B. Vucetic, "Practical physical layer network coding for two-way relay channels: Performance analysis and comparison," *IEEE Trans. Wireless Commun.*, vol. 9, no. 2, pp. 764–777, Feb. 2010.
- [8] R. Zhang, Y. Liang, C. Chai, and S. Cui, "Optimal beamforming for two-way multi-antenna relay channel with analogue network coding," *IEEE J. Sel. Areas Commun.*, vol. 27, no. 5, pp. 699–712, Jun. 2009.
- [9] J. Joung and A. Sayed, "Multiuser two-way amplify-and-forward relay processing and power control methods for beamforming systems," *IEEE Trans. Signal Process.*, vol. 58, no. 3, pp. 1833–1846, Mar. 2010.
- [10] B. Rankov and A. Wittneben, "Spectral efficient protocols for half-duplex fading relay channels," *IEEE J. Sel. Areas Commun.*, vol. 25, no. 2, pp. 379–389, Feb. 2007.
- [11] V. Havary-Nassab, S. Shahbazpanahi, and A. Grami, "Optimal distributed beamforming for two-way relay networks," *IEEE Trans. Signal Process.*, vol. 58, no. 3, pp. 1238–1250, Mar. 2010.
- [12] M. Zeng, R. Zhang, and S. Cui, "On design of collaborative beamforming for two-way relay networks," *IEEE Trans. Signal Process.*, vol. 59, no. 5, pp. 2284–2295, May 2011.
- [13] A. Afana, V. Asghari, A. Ghrayeb, and S. Affes, "Enhancing the performance of spectrum-sharing systems via collaborative distributed beamforming and AF relaying," in *Proc. IEEE GLOBECOM*, Anaheim, CA, USA, Dec. 2012, pp. 1314–1319.
- [14] A. Afana, V. Asghari, A. Ghrayeb, and S. Affes, "On the performance of cooperative Relaying spectrum-sharing systems with collaborative distributed beamforming," *IEEE Trans. Commun.*, vol. 62, no. 3, pp. 857–871, Mar. 2014.
- [15] Q. Li, S. H. Ting, A. Pandharipande, and Y. Han, "Cognitive spectrum sharing with two-way relaying systems," *IEEE Trans. Veh. Technol.*, vol. 60, no. 3, pp. 1233–1240, Mar. 2011.
- [16] L. Yang, M. S. Alouini, and K. Qaraqe, "On the performance of spectrum sharing systems with two-way relaying and multiuser diversity," *IEEE Commun. Lett.*, vol. 16, no. 8, pp. 1240–1243, Aug. 2012.
- [17] A. Afana, A. Ghrayeb, V. Asghari, and S. Affes, "Cooperative two-way selective relaying in spectrum-sharing systems with distributed beamforming," in *Proc. IEEE WCNC*, Shanghai, China, Apr. 2013, pp. 2976–2981.
- [18] A. Afana, A. Ghrayeb, V. Asghari, and S. Affes, "On the performance of spectrum sharing two-way relay networks with distributed beamforming," in *Proc. IEEE SPAWC*, Darmstadt, Germany, Jun. 2013, pp. 365–369.
- [19] K. Zarifi, A. Ghrayeb, and S. Affes, "Jointly optimal source power control and relay matrix design in multipoint-to-multipoint cooperative communication networks," *IEEE Trans. Signal Process.*, vol. 59, no. 9, pp. 4313–4330, Sep. 2011.
- [20] K. Hamdi, K. Zarifi, K. Ben Letaief, and A. Ghrayeb, "Beamforming in relay-assisted cognitive radio systems: A convex optimization approach," in *Proc. IEEE ICC*, Kyoto, Japan, Jun. 2011, pp. 1–5.
- [21] R. Manna, R. H. Y. Louie, Y. Li, and B. Vucetic, "Cooperative spectrum sharing in cognitive radio networks with multiple antennas," *IEEE Trans. Signal Process.*, vol. 59, no. 11, pp. 5509–5522, Nov. 2011.
- [22] K. Jitvanichphaibool, Y.-C. Liang, and R. Zhang, "Beamforming and power control for multi-antenna cognitive two-way relaying," in *Proc. IEEE WCNC*, 2009, pp. 1–6.
- [23] S. H. Safavi, M. Ardebilipour, and S. Salari, "Relay beamforming in cognitive two-way networks with imperfect channel state information," *IEEE Wireless Commun. Lett.*, vol. 1, no. 4, pp. 344–347, Aug. 2012.
- [24] R. Wang, M. Tao, and Y. Liu, "Optimal linear transceiver designs for cognitive two-way relay networks," *IEEE Trans. Signal Process.*, vol. 61, no. 4, pp. 992–1005, Feb. 15, 2013.
- [25] L. Tong, B. M. Sadler, and M. Dong, "Pilot-assisted wireless transmissions: General model, design criteria, signal processing," *IEEE Signal Process. Mag.*, vol. 21, no. 6, pp. 12–25, Nov. 2004.
- [26] L. Zhang, Y.-C. Liang, and Y. Xin, "Joint beamforming and power allocation for multiple access channels in cognitive radio networks," *IEEE J. Sel. Areas Commun.*, vol. 26, no. 1, pp. 38–51, Jan. 2008.
- [27] J. M. Peha, "Approaches to spectrum sharing," *IEEE Commun. Mag.*, vol. 8, no. 1, pp. 10–11, Feb. 2005.
- [28] R. Etkin, A. Parekh, and D. Tse, "Spectrum sharing for unlicensed bands," *IEEE J. Sel. Areas Commun.*, vol. 25, no. 3, pp. 517–528, Apr. 2007.
- [29] L. Musavian, S. Aissa, and S. Lambotharan, "Effective capacity for interference and delay constrained cognitive-radio relay channels," *IEEE Trans. Wireless Commun.*, vol. 9, no. 5, pp. 1698–1707, May 2010.
- [30] A. Basilevsky, *Applied Matrix Algebra in the Statistical Sciences*. New York, NY, USA: North Holland, 1983.
- [31] R. J. Pavur, "Quadratic forms involving the complex Gaussian," Ph.D. dissertation, Math. Dept., Texas Tech Univ., Lubbock, TX, USA, Aug. 1980.
- [32] J. Proakis, *Digital Communications*, 4th ed. New York, NY, USA: McGraw-Hill, 2000.
- [33] M. Simon and M. Alouini, *Digital Communications over Fading Channels*, 2nd ed. Hoboken, NJ, USA: Wiley, 2005.
- [34] I. S. Gradshteyn and I. M. Ryzhik, *Table of Integrals Series and Products*, 7th ed. Amsterdam, The Netherlands: Elsevier, 2007.
- [35] M. Di Renzo, F. Graziosi, and F. Santucci, "A unified framework for performance analysis of CSI-assisted cooperative communications over fading channels," *IEEE Trans. Commun.*, vol. 57, no. 9, pp. 2251–2257, Sep. 2009.

- [36] A. P. Prudnikov, Y. A. Brychkov, and O. I. Marichev, *Integrals and Series, Volume 2,3: Special Functions*. New York, NY, USA: Gordon and Breach, 1988.
- [37] I. Trigui, S. Affes, and A. Stephenne, "Closed-form error analysis of variable-gain multihop systems in Nakagami-m fading channels," *IEEE Trans. Commun.*, vol. 59, no. 8, pp. 2285–2295, Aug. 2011.
- [38] E. Mekic, N. Sekulovic, M. Bandjur, M. Stefanovic, and P. Spalevic, "The distribution of ratio of random variable and product of two random variables and its application in performance analysis of multi-hop relaying communications over fading channels," *Przeglad Elektrotechniczny*, vol. 88, no. 7a, pp. 133–137, 2012 (Electrical Review).
- [39] V. Adamchik and O. Marichev, "The algorithm for calculating integrals of hypergeometric type functions and its realization in reduce systems," in *Proc. Int. Conf. Symbolic Algebraic Comput.*, Tokyo, Japan, 1990, pp. 212–224.
- [40] M. Abramowitz and I. A. Stegun, *Handbook of Mathematical Functions with Formulas, Graphs, Mathematical Tables*, 9th ed. New York, NY, USA: Dover, 1972, pp. 890–923.
- [41] Z. Wang and G. B. Giannakis, "A simple and general parameterization quantifying performance in fading channels," *IEEE Trans. Commun.*, vol. 51, no. 8, pp. 1389–1398, Aug. 2003.
- [42] K. Huang and R. Zhang, "Cooperative feedback for multiantenna cognitive radio networks," *IEEE Trans. Signal Process.*, vol. 59, no. 2, pp. 747–758, Feb. 2011.



Ali Afana received the B.Sc. degree in electrical engineering, major Communications and Control, from the Islamic University of Gaza-Palestine in 2006 and the M.Sc. degree in communications engineering from Birmingham University, Birmingham, UK in 2009 (with Distinction). He is currently working toward his Ph.D. degree in electrical engineering at Concordia University, Montreal, Quebec, Canada. His research interests span different topics in wireless communications, including signal processing for wireless communications, performance analysis of cooperative relaying in cognitive radio networks, and physical-layer security for massive multi-input multi-output (MIMO) systems.



Ali Ghayeb received the Ph.D. degree in electrical engineering from the University of Arizona, Tucson, USA in 2000. He is currently a Professor with the Department of Electrical and Computer Engineering, Texas A&M University at Qatar (on leave from Concordia University, Montreal, Canada.)

He is a co-recipient of the IEEE Globecom 2010 Best Paper Award. He is the coauthor of the book *Coding for MIMO Communication Systems* (Wiley, 2008). His research interests include wireless and mobile communications, error correcting coding, MIMO systems, wireless cooperative networks, and cognitive radio systems.

Dr. Ghayeb has instructed/co-instructed technical tutorials at several major IEEE conferences. He served as the TPC co-chair of the Communications Theory Symposium of IEEE Globecom 2011. He is serving as the TPC co-chair of the 2016 IEEE WCNC conference. He serves as an Editor of the IEEE TRANSACTIONS ON WIRELESS COMMUNICATIONS, and the IEEE TRANSACTIONS ON COMMUNICATIONS. He served as an Associate Editor of IEEE TRANSACTIONS ON SIGNAL PROCESSING, IEEE TRANSACTIONS ON VEHICULAR TECHNOLOGY, the Elsevier Physical Communications, and the Wiley Wireless Communications and Mobile Computing Journal.



Vahid Asghari received the B.Sc. degree in electrical engineering from Azad University in 2002, the M.Sc. degree in telecommunication systems from K.N.Toosi University of Technology in 2005, and the Ph.D. degree in telecommunications from INRS-EMT, University of Quebec, Montreal, Canada in 2012. From 2005 to 2007, he was a Researcher with the department of electrical engineering, K.N.Toosi University of Technology. From 2011 to 2013, he was as a postdoctoral research fellow at INRS-EMT, Montreal, Canada, where he worked on an admission

control algorithm for heterogeneous networks. He is currently working as a postdoctoral research fellow at the department of electrical engineering, McGill University, Montreal, Canada. His research interests include resource scheduling and management, cooperative communications with a focus on heterogeneous systems. He is also interested in behavior modeling, analysis and management of smart applications using ICT technology with a focus on cloud computing networks. He is a recipient of Postdoctoral Research Fellowship Award from the Quebec Government Fonds Québécois de la Recherche sur la Nature et les Technologies (FQRNT), 2012–2014. He is also co-recipient of Best Paper Award from IEEE WCNC 2010.



Sofiene Affes received the Diplome d'Ingenieur in telecommunications in 1992, and the Ph.D. degree with honors in signal processing in 1995, both from Ecole Nationale Supérieure des Telecommunications (ENST), Paris, France. He has been since with INRS, Canada, as a Research Associate until 1997, an Assistant Professor until 2000, and Associate Professor until 2009. Currently he is Full Professor and Director of PERWADE, a unique 4 M\$ research training program on wireless in Canada involving 27 faculty from 8 universities and 10 industrial partners.

Dr. Affes has been twice the recipient of a Discovery Accelerator Supplement Award from NSERC, from 2008 to 2011, and from 2013 to 2016. From 2003 to 2013, he held a Canada Research Chair in Wireless Communications. In 2006, he served as a General Co-Chair of IEEE VTC'2006-Fall, Montreal, Canada. In 2008 he received from the IEEE Vehicular Technology Society the IEEE VTC Chair Recognition Award for exemplary contributions to the success of IEEE VTC. He also received best paper awards at IEEE Globecom'2007, ICASSP'2008, and VTC'2010-Fall. He currently acts as an Associate Editor for three IEEE TRANSACTIONS ON COMMUNICATIONS, Signal Processing, and Wireless Communications, and for the Wiley Journal on Wireless Communications & Mobile Computing.